



Comparison of remotely sensed and modelled soil moisture data sets across Australia



C.M. Holgate^{a, c, *}, R.A.M. De Jeu^b, A.I.J.M van Dijk^a, Y.Y. Liu^c, L.J. Renzullo^d, Vinodkumar^{e, f}, I. Dharsasi^e, R.M. Parinussa^g, R. Van Der Schalie^{b, h}, A. Gevaert^h, J. Walkerⁱ, D. McJannet^d, J. Cleverly^j, V. Haverd^k, C.M. Trudinger^k, P.R. Briggs^k

^aFenner School of Environment Society, The Australian National University, Canberra, Australia

^bVandersat, Noordwijk, Netherlands

^cARC Centre of Excellence for Climate System Science and Climate Change Research Centre, UNSW Australia, Australia

^dCSIRO Land and Water, Australia

^eBureau of Meteorology, Australia

^fBushfire Natural Hazards Cooperative Research Centre, Australia

^gSchool of Civil and Environmental Engineering, UNSW Australia, Australia

^hFaculty of Earth and Life Sciences, VU University Amsterdam, Netherlands

ⁱDepartment of Civil Engineering, Monash University, Australia

^jSchool of Life Sciences, University of Technology Sydney, Australia

^kCSIRO Oceans and Atmosphere, Australia

ARTICLE INFO

Article history:

Received 21 March 2016

Received in revised form 19 August 2016

Accepted 14 September 2016

Available online xxxx

Keywords:

Soil moisture

SMOS

AMSR2

ASCAT

WaterDyn

CABLE

AWRA-L

KBDI

MSDI

API

Comparison

Cluster analysis

In situ

ABSTRACT

This study compared surface soil moisture from 11 separate remote sensing and modelled products across Australia in a common framework. The comparison was based on a correlation analysis between soil moisture products and *in situ* data collated from three separate ground-based networks: OzFlux, OzNet and CosmOz. The correlation analysis was performed using both original data sets and temporal anomalies, and was supported by examination of the time series plots. The interrelationships between the products were also explored using cluster analyses. The products considered in this study include: Soil Moisture Ocean Salinity (SMOS; both Land Parameter Retrieval Model (LPRM) and L-band Microwave Emission of the Biosphere (LMEB) algorithms), Advanced Microwave Scanning Radiometer 2 (AMSR2; both LPRM and Japan Aerospace Exploration Agency (JAXA) algorithms) and Advanced Scatterometer (ASCAT) satellite-based products, and WaterDyn, Australian Water Resource Assessment Landscape (AWRA-L), Antecedent Precipitation Index (API), Keetch-Byram Drought Index (KBDI), Mount's Soil Dryness Index (MSDI) and CABLE/BIOS2 model-based products. The comparison of the satellite and model data sets showed variation in their ability to reflect *in situ* soil moisture conditions across Australia owing to individual product characteristics. The comparison showed the satellite products yielded similar ranges of correlation coefficients, with the possible exception of AMSR2_JAXA. SMOS (both algorithms) achieved slightly better agreement with *in situ* measurements than the alternative satellite products overall. Among the models, WaterDyn yielded the highest correlation most consistently across the different locations and climate zones considered. All products displayed a weaker performance in estimating soil moisture anomalies than the original data sets (*i.e.* the absolute values), showing all products to be more effective in detecting interannual and seasonal soil moisture dynamics rather than individual events. Using cluster analysis we found satellite products generally grouped together, whereas models were more similar to other models. SMOS (based on LMEB algorithm and ascending overpass) and ASCAT (descending overpass) were found to be very similar to each other in terms of their temporal soil moisture dynamics, whereas AMSR2 (based on LPRM algorithm and descending overpass) and AMSR2 (based on JAXA algorithm and ascending overpass) were dissimilar. Of the model products, WaterDyn and CABLE were similar to each other, as were the API/AWRA-L and KBDI/MSDI pairs. The clustering suggests systematic commonalities in error structure and duplication of information may exist between products. This evaluation has highlighted relative strengths, weaknesses, and complementarities between products, so the drawbacks of each may be minimised through a more informed assessment of fitness for purpose by end users.

© 2016 Elsevier Inc. All rights reserved.

* Corresponding author at: Fenner School of Environment Society, The Australian National University, Building 141, Linnaeus Way, Canberra, ACT 2601, Australia.
E-mail address: chiara.holgate@anu.edu.au (C. Holgate).

1. Introduction

The importance of soil moisture as an environmental variable is evident from its key role in the hydrological cycle. Soil moisture influences rainfall-runoff processes, infiltration, groundwater recharge, and constrains evapotranspiration and photosynthesis. It thus partly governs water and energy exchanges between the land, vegetation and the atmosphere (Albergel et al., 2012; Brocca et al., 2011; Su et al., 2013; Taylor et al., 2012) and influences multi-scale feedbacks (Seneviratne et al., 2010). Understanding how soil moisture varies in time and space is essential for producing environmental forecasts and improving their predictions (Draper, 2011; Owe et al., 2008).

The relevance of soil moisture is also evident in the growing number of applications employing soil moisture data around the world. Some applications include: assimilation into land surface models (e.g. Renzullo et al., 2014) for numerical weather forecasting (e.g. Draper et al., 2009, Dharssi et al., 2011), national water accounting (e.g. Viney et al., 2014) and bushfire danger warning (e.g. Van Dijk et al., 2015; Finkele et al., 2006, Kumar et al., in press), as well as evaluation of regional climate indices and long-term hydrological trends (e.g. Brocca et al., 2014; Liu et al., 2009; Liu et al., 2007), evaluation and improvement of convective processes in climate models (Taylor et al., 2012), drought monitoring and evaluation (e.g. Van Dijk et al., 2013; Pozzi et al., 2013), and flood prediction (e.g. Wanders et al., 2014), among others. Many of these applications have been or are currently being employed in Australia in an effort to better understand and predict the water resources of a country with long-standing climatic variability.

There are several operational or near-operational sources of soil moisture information for Australia. Sources of soil moisture information are generally from one of three broad categories: *in situ* measurements, satellite remotely sensed estimates, and model predictions. Ground-based approaches measure *in situ* soil moisture at a point scale using techniques that utilise the dielectric constant of the soil (e.g. time domain reflectometry (TDR) and soil capacitance measurements) or matric potential of the soil (e.g. tensiometer and resistance unit measurements) typically on a sub-daily time step. Alternatively *in situ* measurements may also be taken over a broader scale (tens of hectares) using cosmic-ray neutron detectors, also on a sub-daily time step. Remotely sensed soil moisture estimates may be obtained on an even larger scale (tens or hundreds of square kilometres) from a growing number of satellite platforms that are able to provide data on a daily basis or every few days. Active or passive satellite instruments operating in the microwave bands are suited to the acquisition of soil moisture due to the large contrast in the dielectric constant between water and soil (Schmugge, 1983). Several radiative transfer models and a change detection algorithm have been developed (e.g. Maeda and Taniguchi, 2013, Owe et al., 2001, Wagner et al., 1999) to retrieve soil moisture from the microwave and radar measurements and are currently in use.

Soil moisture may also be estimated through land surface schemes or hydrological models, with spatial and temporal resolution depending on model structure and purpose. The accuracy of the modelled soil moisture is significantly influenced by the accuracy and spatial coverage of the input precipitation and soil hydraulic property data, in addition to the adequacy of the model structure and assumptions. Soil moisture data sets from remotely sensed and modelled sources are systematically different in the way they estimate soil moisture, and may be better suited to some climatic and environmental conditions than others. The objective of this study is therefore to answer the following research questions:

1. How do currently used remotely sensed and modelled products of surface soil moisture compare across Australia, and what are the driving processes?

2. Which products are most similar to each other and demonstrate similar error structures?

A number of previous studies have compared satellite and/or modelled soil moisture with *in situ* data within Australia (e.g. Brocca et al., 2014, Renzullo et al., 2014, Liu et al., 2009). Although the agreement between the data sets may be well established for the locations of the *in situ* stations, previous efforts have mainly focused on ground data from south-eastern Australia, such as the Murrumbidgee River catchment (e.g. Van der Schalie et al., 2015; Panciera et al., 2014; Dorigo et al., 2015; Su et al., 2013; Yee et al., 2013; Albergel et al., 2012; Mladenova et al., 2011; Draper et al., 2009) where a network of *in situ* stations are located, and often cover relatively short observation periods.

In light of the increasing number of important applications that utilise soil moisture data, the increasing number of approaches for its estimation, and the often limited geographical area, time frame and range of climate zones in previous studies, this study builds upon previous comparisons carried out over Australia in several ways.

Firstly, the coverage of *in situ* locations used as a reference for comparison is enlarged by extending the number of stations to include three separate networks, which include the emergent cosmic-ray technology as well as more traditional TDR and frequency-domain sensors. The networks include OzFlux (e.g. Cleverly, 2011), OzNet (Smith et al., 2012) and CosmOz (Hawdon et al., 2014), which when combined provide *in situ* soil moisture information over a broader range of geographies and climate zones across Australia than any of the networks individually. The entire time period of available data for all networks is considered, beginning with the earliest data (2001) and continuing through 2014.

Secondly, this study collates soil moisture data from multiple relevant sources, which hitherto have not been compared in a single study, across both model and remote sensing platforms. Collation of these different sources of soil moisture data in this comparison has allowed them to be viewed side by side and evaluated in a common framework. Also within individual remote sensing platforms, data sets developed with different radiative transfer algorithms by different research teams are considered.

Thirdly, the interrelationships between the products themselves are explored through cluster analyses. Addressing these research questions will provide a more detailed understanding of the strengths and weaknesses of a number of soil moisture products and further the appreciation of complementarity between sources, allowing the drawbacks of each to be minimised through a more informed assessment of fitness for purpose.

2. Materials

2.1. *In situ* data

The *in situ* data collated for this study forms the reference for comparison with satellite and model derived soil moisture estimates. *In situ* data were obtained and processed from three separate networks: OzFlux, OzNet and CosmOz (Fig. 1). Data from the combined *in situ* network are available for a range of time periods, beginning in 2001.

While *in situ* data has been used as a reference for comparison in this study, the point measurements that largely comprise the data set may or may not be representative of a wider spatial footprint across the landscape as seen by satellite and model products. Which source of soil moisture data may be considered as the 'truth' is debatable. To compare satellite and model products of soil moisture across different regions of Australia, it is practical to utilise a ground-based network as a reference, where a multi-year record of calibrated soil moisture observations is available within most climate regions across Australia.

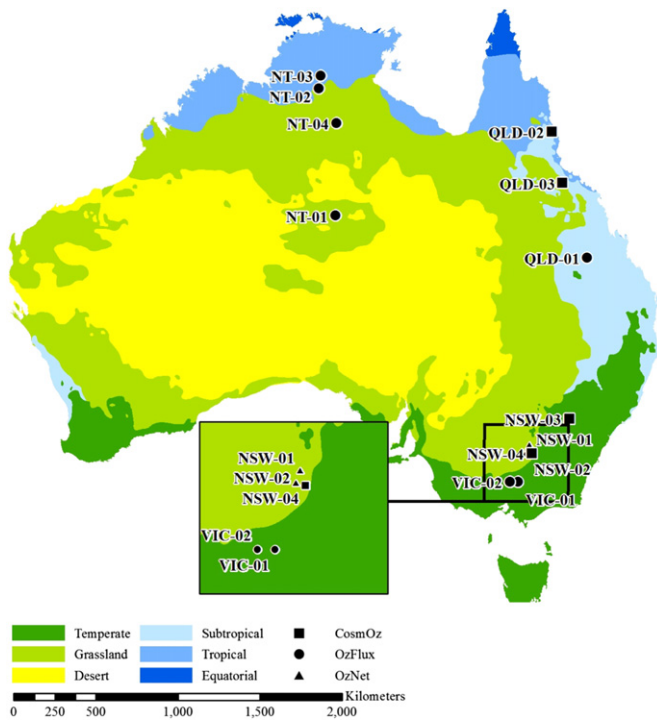


Fig. 1. *In situ* network station locations with major Köppen climate zones (Bureau of Meteorology, 2012).

Soil moisture is measured differently between the networks, and is further described in the following sections. While the systematic differences in measurement approach add complexity to the comparative analysis, the three networks can complement each other when comparing to soil moisture estimated from satellite and model products. For instance the shallower observation depths of the OzNet and OzFlux networks are more comparable to the shallow observation depths of satellites and models; yet the dependence of satellite observation depth with time, mainly depending on soil wetness conditions (e.g. Jackson et al., 2012; see Sections 2.2 and 2.3), is more like the behaviour of the CosmOz sensors. Furthermore the measurement footprint of the CosmOz stations is closer to that of satellite footprints than the point measurements of the OzNet and OzFlux networks. Such systematic differences may be evident from the comparison.

The inclusion of data from an *in situ* station was based on several criteria. Firstly, *in situ* measurements must be available within the study time period (1 January 2001 to 31 December 2014) as well as the shorter period of July 2012 to July 2013, which is common to the satellite and model products. Secondly, station locations were used where the number of coincident daily data points between the *in situ* and time series from all products was greater than or equal to 10 data points per season in both the longer and common periods of comparison. This is to ensure a correlation is made between the *in situ* station and *all* products at a given location, based on data from all seasons. Lastly, the data needed to be publicly available. Table 1 provides an overview of the *in situ* stations meeting these criteria and subsequently focused on in this study. The *in situ* stations considered span a range of environments, situated across wetter and drier areas (annual average rainfall ranged between 175 and 700 mm/year) and multiple climate zones (tropical, sub-tropical, grassland and temperate; Table 1). For this study sites have been named based on the state or territory they reside in, i.e. the Northern Territory (NT), Queensland (QLD), New South Wales (NSW) and Victoria (VIC).

2.1.1. OzFlux

OzFlux is part of a global network of over 500 micrometeorological stations worldwide that provide energy, carbon and water exchange observations with the atmosphere and numerous ecosystem types (www.ozflux.org.au; Baldocchi, 2008). In Australia, OzFlux consists of approximately 37 stations, of which 30 are currently active. Profile soil moisture in the OzFlux network is measured at individual stations using frequency-domain reflectometers (generally Campbell Scientific CS-616 (USA) probes) every 30 min. Data are provided at four levels of processing. Level 3 data has been subject to detailed quality control and has been used in this study. Data sets were downloaded directly from the OzFlux data portal (data.ozflux.org.au/portal) with soil moisture data given in volumetric units. Data from the OzFlux network were publicly available at 22 of the 37 stations across Australia, including 20 active stations and two stations which are no longer operational. Of these 22 stations, seven provided soil moisture data in the topsoil's upper 10 cm and met the criteria for inclusion.

2.1.2. OzNet

OzNet contains 63 monitoring stations within its network spanning the 82,000 km² Murrumbidgee River catchment in south-eastern Australia (Smith et al., 2012; http://oznet.org.au). All monitoring stations measure soil moisture, soil temperature and rainfall (Smith et al., 2012), every 20 to 30 min. The first stations were installed in 2001 and focused on root-zone soil moisture measurement (profile to a depth of 90 cm), with later installations measuring the top 0–5 cm (Smith et al., 2012). The older stations use Campbell Scientific (USA) water content reflectometers, and convert to volumetric soil moisture using calibration equations involving soil type and temperature information. The newer stations utilise Stevens Hydraprobe (USA) sensors, inferring volumetric soil moisture from the dielectric constant and conductivity measured (Merlin et al., 2007). Within the OzNet monitoring network two stations satisfied the applied criteria for inclusion.

2.1.3. CosmOz

CosmOz is a network of cosmic-ray sensors currently installed and operating (and calibrated) at nine locations around Australia. Each location houses a CRP-1000b Hydroinnova (USA) cosmic-ray sensor, which counts fast neutrons produced by cosmic rays passing through the earth's atmosphere (Hawdon et al., 2014). The probes are located approximately 2 m above ground and count neutrons in the soil and air above it (Hawdon et al., 2014). The fast neutron count is primarily controlled by the soil water content, where neutrons are moderated by hydrogen atoms within the water molecule. Thus the lower the neutron count, the more scattering that has taken place and the higher the soil moisture, and *vice versa*. Neutron count is corrected for several processes such as the effect of atmospheric pressure, vapour pressure changes and the variation in incoming neutron intensity (Hawdon et al., 2014). Neutron counts can also be affected by water in the vegetation surrounding the probe. In the CosmOz network, the effect of vegetation water on neutron count is effectively eliminated by calibrating each probe to local soil moisture conditions, assuming the hydrogen pool in the vegetation remains stable. This is considered a reasonable assumption for the sites of interest in this study and time period. Once corrections have been made, the neutron count is converted to volumetric soil moisture using a calibration function (Desilets et al., 2010) which is adjusted to known wet and dry soil moisture conditions.

Hourly soil moisture time series data were obtained from Hawdon et al. (2014) (http://cosmoz.csiro.au) for this study at four locations (Table 1) consistent with the *in situ* selection criteria.

Table 1
Summary of *in situ* stations.

Site name	Network name	Location	Data period	Depth [cm]	Köppen climate zone	Land type	MAR ^a [mm]	MATR ^b [° C]	Reference	
OzFlux	NT-01	Alice Springs Mulga	22.3S, 133.2E	2010–2013	0–10	Grassland	Semi-arid mulga	260	7–35	Cleverly (2011)
	NT-02	Dry River	15.3S, 132.4E	2008–2013	0–5	Grassland	Open forest savannah	560	14–36	Beringer (2013)
	NT-03	Red Dirt Melon Farm	14.6S, 132.5E	2011–2013	0–5	Tropical	Tropical savannah	600	17–33	Beringer (2014)
	NT-04	Sturt Plains	17.2S, 133.4E	2008–2013	0–5	Grassland	Grassy plain	670	12–36	Beringer (2013a)
	QLD-01	Arcturus Emerald	23.9S, 148.5E	2011–2013	0–5	Subtropical	Pasture	520	9–34	Schroder (2014)
	VIC-01	Riggs Creek	36.6S, 145.6E	2010–2013	0–5	Temperate	Pasture	310	5–34	Beringer (2014a)
	VIC-02	Whroo	36.7S, 145.0E	2011–2013	0–10	Temperate	Box woodland	575 ^c	5–32	Beringer (2013b); Bureau of Meteorology (2016)
	OzNet	NSW-01	Y2	34.7S, 146.1E	2003–2014	0–5	Grassland	Dryland cropping	210	–1–43 ^c
NSW-02		Y9	35.0S, 146.0E	2003–2014	0–5	Grassland	Dryland cropping	345	–1–43 ^c	Smith et al. (2012); Bureau of Meteorology (2016a)
CosmOz	NSW-03	Baldry	32.9S, 148.5E	2011–2014	Variable	Temperate	Pasture	700	–1–42 ^c	CSIRO (2015); Bureau of Meteorology (2016b)
	NSW-04	Yanco	35.0S, 146.3E	2011–2014	Variable	Grassland	Grazed	175	–1–43 ^c	CSIRO (2015); Bureau of Meteorology (2016a)
	QLD-02	Robson	17.1S, 145.6E	2010–2014	Variable	Subtropical	Tropical rainforest	510	7–37 ^c	CSIRO (2015); Bureau of Meteorology (2016c)
	QLD-03	Weany	19.9S, 146.5E	2010–2014	Variable	Grassland	Grazed open woodland	650	4–41 ^c	CSIRO (2015); Bureau of Meteorology (2016d)

^a MAR = mean annual rainfall at the site over the stated data period.

^b MATR = mean annual temperature range at the site over the stated data period.

^c Data from nearest BOM station for the stated data period, with MATR defined as the range between the mean minimum and mean maximum annual values.

2.2. Satellite data

2.2.1. SMOS

The Soil Moisture Ocean Salinity (SMOS) satellite launched in November 2009 carries the Microwave Imaging Radiometer with Aperture Synthesis (MIRAS) radiometer that operates in the L-band, utilising a single channel at 1.4 GHz to estimate volumetric soil moisture to approximately 5 cm depth (Kerr et al., 2010), increasing or decreasing mainly depending on lower or higher soil moisture content. The Y-shaped instrument carries 69 regularly spaced dual-polarisation antennas that achieve an average spatial resolution of approximately 43 km, sampling the earth once every 3 days (Kerr et al., 2010). SMOS has an equatorial crossing time of 0600 h (ascending) and 1800 h (descending) local time.

In this study two SMOS products have been utilised. Firstly, the official product of volumetric soil moisture ‘SMOS_LMEB’ (version RE04) was obtained from the Centre Aval de Traitement des Données SMOS (CATDS), operated for the Centre National d’Etudes Spatiales (CNES, France) by IFREMER (Brest, France) for the period 15 January 2010 to 31 December 2014 (see <http://catds.ifremer.fr/Products>). Secondly, volumetric soil moisture estimates derived by the Land Parameter Retrieval Model (LPRM) algorithm for the period 1 July 2010 to 31 December 2014 were obtained from Van der Schalie et al. (2016), here named ‘SMOS_LPRM’.

The LPRM is a forward radiative transfer model that uses both horizontally and vertically polarised microwave brightness temperatures to partition the detected surface emission into soil and vegetation components using an analytical solution by Meesters et al. (2005). The model is run iteratively, varying the soil moisture term until the simulated brightness temperature converges with the observed. Once the model has converged, a dielectric mixing model (Wang and Schmugge, 1980) and a global database of soil physical properties (Rodell et al., 2004) are applied to determine the absolute soil moisture values (Owe et al., 2001). The official LMEB product similarly uses an iterative forward radiative transfer model. The main

point of difference between the two algorithms is the classification of land cover types within the footprint (estimated from high resolution land use maps) that are used to estimate the contribution of each cover type to the surface microwave emission (Wigneron et al., 2007) in the LMEB approach. Furthermore, the official LMEB algorithm constrains the model based on changes to vegetation optical thickness as measured by overpasses in a given time period (Kerr et al., 2012).

Both the SMOS_LPRM and SMOS_LMEB products were provided as volumetric soil moisture estimates on a global 25 km Equal Area Scalable Earth 2 (EASE2) grid with a cylindrical equal area projection. Each data set was resampled to a daily $0.25^\circ \times 0.25^\circ$ regular grid and quality controlled using flags for open water, snow, frost and coastal areas. The SMOS_LMEB data set was also filtered using the associated SMOS level 3 data quality control index, retaining soil moisture estimates with an uncertainty below $0.06 \text{ m}^3/\text{m}^3$.

2.2.2. AMSR2

The Advanced Microwave Scanning Radiometer 2 (AMSR2) instrument on board the Japan Aerospace Exploration Agency (JAXA) Global Change Observation Mission - Water 1 (GCOM-W1) satellite was launched in May 2012 into the A-Train satellite constellation. The AMSR2 instrument contains seven dual polarised frequency channels centred at 6.9, 7.3, 10.7, 18.7, 23.8, 36.5 and 89.0 GHz (Imaoka et al., 2010). The C-band (6.9 and 7.3 GHz) and X-band frequencies (10.7 GHz) are utilised for volumetric soil moisture estimation at a spatial resolution of approximately 50 km (Imaoka et al., 2010), sensitive to the top 1–2 cm of soil (Escorihuela et al., 2010, Owe et al., 2008). AMSR2 has an equatorial overpass time of 1330 h (ascending) and 0130 h (descending) local time, with near complete earth coverage approximately every two days.

In this study soil moisture data from two different retrieval algorithms were obtained: the official JAXA soil moisture product (here named ‘AMSR2_JAXA’) utilising X-band retrievals, and the soil moisture product derived using the LPRM (here named ‘AMSR2_LPRM’) for both the C-band and X-band retrievals. The JAXA algorithm is

a forward radiative transfer model that simulates brightness temperatures under various combinations of land parameters (such as vegetation signal attenuation and optical depth properties; fraction of pixel covered by vegetation) to develop look-up tables of soil moisture and vegetation water content (Maeda and Taniguchi, 2013; Jackson et al., 2010). The JAXA algorithm has been calibrated to *in situ* data obtained in south-eastern Australia, Mongolia and Thailand (Maeda and Taniguchi, 2013).

The AMSR2_JAXA product was obtained from JAXA GCOM-W1 Data Providing Service (<https://gcom-w1.jaxa.jp/auth.html>) for the period 3 July 2012 to 31 December 2014. Product version 1.1 has been used in this study (the most recent version 2.0 was not available for the whole study period). The AMSR2_LPRM volumetric soil moisture data were obtained from Parinussa et al. (2015) for the period 2 July 2012 to 31 December 2014. Both products were provided as daily volumetric soil moisture estimates on a global $0.25^\circ \times 0.25^\circ$ regular grid, quality controlled for open water, frozen conditions and coastal areas.

2.2.3. ASCAT

The Advanced Scatterometer (ASCAT) instrument on board the Meteorological Operational-A (Metop-A) satellite was launched in October 2006, and is a real aperture radar with six sideways-looking antennae operating in the C-band (5.3 GHz) with a vertical polarisation (Wagner et al., 2013).

ASCAT measurements are available at spatial resolutions of 50 km and 25 km (Wagner et al., 2013), with global coverage achieved approximately every 1.5 days. Measurements are taken over Australia approximately twice a day (Su et al., 2013) with an equatorial crossing time of 2130 h (ascending) and 0930 h (descending) local time (Wagner et al., 2013). ASCAT is a radar instrument that measures the backscatter of transmitted C-band pulses (Wagner et al., 2013). The production and subsequent retrieval of the backscattered signal is what makes ASCAT an 'active' satellite platform, as distinguished from the previous satellites which 'passively' detect radiation upwelling from the earth's surface.

The six antennae (three either side) of Metop-A provide three independent measurements of backscatter coefficients, which allows radar backscatter at different incidence and azimuth angles to be registered (Wagner et al., 1999a). The influence of soil moisture can be observed from the backscatter observations by removing the effect of vegetation through the employment of a time series based change detection algorithm, developed by Wagner et al. (1999). The effect of vegetation is removed by estimating the typical yearly phenological cycles around the world (Brocca et al., 2011). Surface roughness also has a strong influence on backscatter values (Wagner et al., 2013; Verhoest et al., 2008) but is assumed to remain constant in time (Brocca et al., 2011). In this algorithm the backscatter, extrapolated to a reference angle of 40° , is scaled based on the minimum and maximum historical values (Albergel et al., 2012). Assuming land cover remains relatively static over long periods of time changes are attributed to variations in soil moisture, yielding soil moisture in relative terms (Wagner et al., 2013). A time series of relative soil moisture is then obtained between 0% (dry) and 100% (wet) of reference conditions, for a depth of less than 2 cm (Wagner et al., 2013; Schmugge, 1983). The reference 'dry' and 'wet' values are estimated from extremes in backscatter measurements taken between August 1991 and May 2007 (Naeimi et al., 2009).

The 25 km operational resolution soil moisture product (here named 'ASCAT_TUW') on a discrete global grid produced by Vienna Institute of Technology (<http://rs.geo.tuwien.ac.at/products/surface-soil-moisture/ascat/>) was used in this study for the period 1 January 2007 to 31 December 2013. The data were resampled to a daily $0.25^\circ \times 0.25^\circ$ regular grid commensurate with the other satellite data sets, and quality controlled for open water, frozen conditions and coastal areas.

2.3. Model data

The models considered in this study have been developed by a number of research teams and are diverse in approach and purpose. Inevitably different modelling approaches lead to different representations of soil moisture, and with estimations made at different depths and times. This reality is reflected in the range of products considered in this study, all of which are currently utilised in Australia for various purposes. In an effort to limit the impact of model estimates at different times and depths on the assessment, an additional period common to all products is considered, as well as an additional and deeper uniform depth where possible.

Despite differences in model approach, all models considered in this study share common precipitation forcing prepared by Jones et al. (2009) as part of the Australian Water Availability Project (AWAP). The gridded data set contains daily precipitation at 0.05° resolution and is based solely on interpolated station data. The accuracy of the spatial product was assessed through a cross-validation procedure which repeatedly deleted 5% of stations at a time and the error in the analysis of the remaining stations calculated (Jones et al., 2009). For the period 2001–2007 the daily rainfall values have a root mean square error of 3.1 mm and a mean absolute error of 0.9 mm (Jones et al., 2009). In the context of this study common precipitation forcing among model products is seen as an advantage, as precipitation is a key driver of soil moisture variability and therefore differences between products may instead be related to other model-specific factors.

2.3.1. WaterDyn

The AWAP project, developed by the Commonwealth Scientific and Industrial Research Organisation (CSIRO), the Australian Bureau of Meteorology (BOM) and the Australian Bureau of Agricultural and Resource Economics and Sciences, implements a continental-scale water balance over Australia using the WaterDyn model at a resolution of 0.05° (Raupach et al., 2009).

Water balance calculations are carried out for two spatially-varying soil layers: a shallow soil layer with thicknesses ranging from 8 to 70 cm (typically 20 cm at the sites considered in this study), and a lower layer with thicknesses between 50 and 190 cm, depending on soil type (Raupach et al., 2009; Briggs, 2016, pers. comm). In this study estimates from the upper soil layer are considered. The mass balance of water flux across the boundaries of the upper layer is estimated based on a precipitation input, and a combined output from transpiration, soil evaporation, surface runoff and drainage to the deeper layer (Raupach et al., 2009). An estimate of relative water content is then made based on the saturated volumetric water content and depth of the layer.

Time series of daily average relative soil water content (between 0 and 1) for the whole of Australia were obtained for this study for the period 1 January 2001 to 31 December 2013, based on AWAP WaterDyn model version 26M.

2.3.2. CABLE

The CSIRO Atmosphere Biosphere Land Exchange (CABLE) is a land surface scheme that simulates coupled carbon and water cycles and was configured here on a 0.05° grid. For this study volumetric soil moisture estimates were extracted from a modified version of CABLE in the BIOS2 modelling environment (Haverd et al., 2013). In BIOS2, the soil and carbon modules of CABLE v1.4 were replaced by the SLI soil model (Haverd and Cuntz, 2010) and CASA-CNP biogeochemical model (Wang et al., 2007), respectively (Haverd et al., 2013). CABLE/BIOS2 was forced with soil data mapped in the Digital Atlas of Australian Soils (Northcote et al., 1960, 1975); and vegetation cover of each grid cell, which was subdivided into woody and grassy vegetation and assigned a Leaf Area Index (LAI; Haverd et al., 2013).

The model was run at an hourly timestep between 1990 and 2014, with the period 1990–2000 used to initialise soil moisture. The model defines 10 soil layers including 0–2.2 cm, 2.2–8 cm, 8–15 cm, 15–30 cm, 30–60 cm, 60–90 cm, 90–120 cm, 120–240 cm, 240–540 cm and 540–990 cm. To compare with *in situ* measurements, soil moisture estimates from the shallowest two model layers have been aggregated using a weighted arithmetic mean to produce a time series for the 0–8 cm layer.

2.3.3. AWRA-L

The Australian Water Resource Assessment (AWRA) system was developed by BOM and CSIRO as part of an effort to deliver comprehensive water accounting information across the country (Vaze et al., 2013; Stenson et al., 2011). The AWRA landscape model (AWRA-L) is a grid-based distributed biophysical model of the water balance between the atmosphere, soil, groundwater and surface water stores (Viney et al., 2015). AWRA-L estimates a daily running water balance on a $0.05^\circ \times 0.05^\circ$ grid across Australia (Viney et al., 2015) commensurate with meteorological forcing data sourced from AWAP.

The water balance is computed for each grid cell for two hydrological response units: shallow-rooted vegetation and deep-rooted vegetation (Viney et al., 2015). The unsaturated zone is partitioned into three layers, each with a maximum spatially varying water holding capacity: top layer (0–10 cm), shallow root zone layer (10–100 cm) and a deep root zone layer (100–600 cm). Water enters the top soil layer as net precipitation (precipitation minus interception) and may leave as soil evaporation, surface runoff or drainage through to deeper layers (Viney et al., 2015).

In this study the AWRA-L (version 5) water storage values [mm] from the top layer (0–10 cm) have been utilised. In order to evaluate soil moisture estimates alongside the other products, the AWRA-L water storage estimates have been scaled between local minimum and maximum values to produce a time series of relative soil wetness values between 0 and 1 for the period 1 January 2001 to 31 December 2014.

2.3.4. API

The Antecedent Precipitation Index (API) is an empirical relation describing soil wetness conditions that has historically been utilised in rainfall-runoff calculations (Choudhury and Blanchard, 1983; Kohler and Linsley, 1951). API has been used in the past to estimate catchment wetness conditions prior to storm events given the strong influence of soil wetness on runoff generating processes and the difficulty in accurately measuring soil moisture over large areas. The API is commonly of the form shown in Eq. (1).

$$API_t = \gamma API_{t-1} + P_t \text{ [mm]} \quad (1)$$

The index of the preceding day (API_{t-1}) [mm] is multiplied by a recession coefficient (γ) [–], and P_t [mm] is the amount of rainfall recorded on day (t) the index is to be calculated. The recession coefficient is a measure of the decline of the influence of past precipitation (Kohler and Linsley, 1951), *i.e.* the decline in memory of the soil column. The recession coefficient of the product used in this study was represented by the function:

$$\gamma = 0.85 + \delta(20 - T_{max,t}) \text{ [–]} \quad (2)$$

where $T_{max,t}$ is the maximum daily temperature [$^\circ\text{C}$] and δ is a sensitivity parameter [$^\circ\text{C}^{-1}$] (Crow et al., 2005). The API data set was generated by Kumar et al. (in press) on a daily time step for the whole of Australia on a $0.05^\circ \times 0.05^\circ$ grid for the period 1 January 2012 to 31 December 2014. Since API values are precipitation depths, the time series was scaled to the local minimum and maximum values to produce a data set of relative soil wetness between 0 and 1. API

is simply a proxy representing soil moisture due to a precipitation depth, and does not relate to a specific soil column depth.

2.3.5. KBDI

The Keetch-Byram Drought Index (KBDI; Keetch and Byram, 1968) is an empirical relation describing the cumulative soil moisture deficit of shallow soil layers. KBDI is currently in use in some parts of Australia as part of a suite of tools used to predict and manage bushfire hazard. KBDI is a simplified, running, daily water balance where soil moisture deficit (SMD) is determined by the difference between the daily effective rainfall ($P_{eff,t}$) and daily evapotranspiration (ET_t), as shown by Eq. (3).

$$SMD_t = SMD_{t-1} - P_{eff,t} + ET_t \text{ [mm]} \quad (3)$$

$P_{eff,t}$ [mm] is the portion of rainfall falling on a catchment that infiltrates into the soil, and is lessened by a constant 5 mm of the first part of an event (Finkele et al., 2006). ET_t [mm] is calculated through an empirical equation which is controlled by the previous day's KBDI value (SMD_{t-1}), the previous day's maximum temperature and the mean annual rainfall (Finkele et al., 2006). Conceptually ET is expected to be a function of vegetation density, which is itself considered to be an exponential function of mean annual rainfall (Keetch and Byram, 1968).

The SMD_{t-1} [mm] calculated through the running water balance represents the amount of water required to bring the soil column back to field capacity, and ranges between 0 and 200 mm (Finkele et al., 2006). The value of 200 mm comes from the original depth of water selected by Keetch and Byram (1968) to represent the field capacity of a soil profile depth where drought events are thought to have a clear impact on bushfire hazard. The actual depth of soil this represents thus depends on the soil type, where a greater depth would be represented in a sandy soil for example, compared to a clayey soil with a higher porosity. For this study the converse of the soil moisture deficit has been scaled to its local minimum and maximum values to produce a relative soil moisture time series between 0 and 1 (*i.e.* 200 mm deficit at wilting point = 100% deficit = 0% soil moisture; 0 mm deficit at field capacity = 0% deficit = 100% soil moisture).

KBDI values have been generated by Kumar et al. (in press) for the period 1 January 2001 to 31 December 2014 using rainfall and temperature data from AWAP on a daily time step for the whole of Australia on a $0.05^\circ \times 0.05^\circ$ grid.

2.3.6. MSDI

Mount's Soil Dryness Index (Mount, 1972) is a similar empirical relation to KBDI in that it is a cumulative soil moisture deficit index, and is also currently used in Australia for bushfire hazard management. MSDI is represented by the same formula as KBDI (see Eq. (3)), but differs in its determination of the P_{eff} and ET terms. To estimate ET the MSDI model assumes a linear relation between mean monthly pan evaporation and mean monthly maximum temperature data measured in Australian capital cities. To calculate $P_{eff,t}$ and partition precipitation into infiltration, runoff or interception, the MSDI model considers the type of vegetation present and assigns each vegetation class their own values of canopy interception, canopy storage, wet evaporation rates and a flash runoff fraction Finkele et al. (2006). For the data set used in this study the vegetation type of each model cell has been estimated through a linear relationship between vegetation class and leaf area index detailed in Finkele et al. (2006). Like the KBDI data set, the converse of the MSDI soil moisture deficit has been scaled to its local minimum and maximum values to produce a relative soil moisture time series. The MSDI time series has been generated by Kumar et al. (in press) for the period 1 January 1974 to 31 December 2014 using rainfall and temperature data from AWAP

on a daily time step for the whole of Australia on a $0.05^\circ \times 0.05^\circ$ grid.

3. Methodology

Direct comparison between the *in situ* data and the satellite and model soil moisture products is challenging due to the systematic differences between each data source. Soil moisture measurements differ in terms of (a) observation depth, (b) temporal change of the observation depth, (c) horizontal support and (d) sampling frequency. For instance the fixed observation depth of the OzNet and OzFlux networks (often taking measurements at several integrated depths, including measurements from the top 0–10 cm or 0–5 cm of soil) contrasts with the variable depth of the CosmOz sensors, which vary in their observation depth depending on soil conditions (Hawdon et al., 2014; Zreda et al., 2008; Franz et al., 2012) and in this study typically vary between 0–7 and 0–50 cm. These contrast with the typical observation depth of the top ≈ 1 –5 cm as seen by satellites, depending on wavelength, soil conditions, moisture content and cover (Kerr et al., 2010; Owe et al., 2008).

Contrasts exist between the point scale measurement of the OzNet and OzFlux networks and the intermediate spatial scale of the CosmOz network. The horizontal support of the cosmic-ray probes is a circle of approximately 600 m diameter around the probe, *i.e.* approximately 30 ha (Hawdon et al., 2014). Furthermore the model and satellite products represent estimates over tens of square kilometres. Analysis of comparison between products with different spatial support is further complicated by soil moisture variability being controlled by the processes at play at different scales (Vinnikov et al., 1999), and at different levels of wetness (Brocca et al., 2014).

Lastly, soil moisture measurements differ in their sampling frequency, and in the networks considered in this study range from 20 min in the OzNet network, to 30 min in the OzFlux network, to hourly in the CosmOz network.

Compounding these issues of scale are the different sources of uncertainty and error associated with each data source. These systematic differences prevent absolute agreement between the different products (Brocca et al., 2011; Draper et al., 2009).

For these reasons the comparisons of satellite and model products are based on their relative temporal agreement with the *in situ* data, using the Pearson correlation coefficient as the primary statistical metric. From this, four methods were implemented to compare the satellite and model products to the *in situ* measurements to assess their relative performance across Australia, and potential interrelationships, and are outlined in the sections following.

3.1. Pearson correlation coefficient

The degree of association between the *in situ* reference data and product data sets was calculated using the Pearson correlation coefficient (R) according to Eq. (4).

$$R = \frac{\frac{1}{n} \sum_{t=1}^n (\theta_{t,p} - \bar{\theta}_p)(\theta_{t,i} - \bar{\theta}_i)}{\sqrt{\frac{1}{n} \sum_{t=1}^n (\theta_{t,p} - \bar{\theta}_p)^2 \frac{1}{n} \sum_{t=1}^n (\theta_{t,i} - \bar{\theta}_i)^2}} \quad (4)$$

$\theta_{t,p}$ and $\theta_{t,i}$ refer to the daily average soil moisture of a product (p ; either satellite or model) and *in situ* (i) respectively, and $\bar{\theta}_p$ or $\bar{\theta}_i$ its average over the time series from $t = 1$ to n days. Correlations were only performed when at least 10 coincident data points each season were present between the reference *in situ* data set and the comparison product, to ensure a sufficient sample size in determining if the

calculated correlation is likely to be different from zero. At stations where this threshold was met or exceeded, correlation analysis was performed using the maximum number of coincident observations in the study time period (1 January 2001 to 31 December 2014), as well as in a shorter period (July 2012 to July 2013). The longer period allowed interannual cycles to be studied with multi-year climatology. The shorter time period was chosen to constrain the correlation to a period common to all products. By studying both the longer and common periods, the correlation analysis avoids being strongly influenced by data gaps and the inclusion or exclusion of extreme events (Loew, 2014). In both cases the correlation statistic was only analysed at sites where the entire seasonal cycle was observed. The significance of each correlation was also calculated using a p -value of 0.01.

The data from each *in situ* station were transformed into a time series of daily averages, bringing the range of measurement frequencies into a common format. This time series of daily *in situ* soil moisture for the study time frame forms the reference for comparison with other products.

Each satellite soil moisture product was resampled to a common $0.25^\circ \times 0.25^\circ$ regular grid. The satellite pixel whose centroid is co-located with each *in situ* station coordinate on the grid was chosen and the corresponding daily soil moisture time series extracted. Where several satellite pixels fall within the reprojected grid cell the arithmetic average was taken. Soil moisture data from each of the models were provided as daily time series at the location coordinates of the *in situ* stations. In this way time series of daily soil moisture values were compiled at each station for each of the *in situ*, satellite and model estimates.

Product soil moisture estimates have not been weighted to specific depth fractions of overlap with the *in situ* measurements, since most products provide soil moisture estimates at depths varying with soil conditions (*i.e.* all but the WaterDyn, CABLE and AWRA-L products). To compare the different products the correlation has been calculated between *in situ* measurements (for measurement depths listed in Table 1) and product soil moisture estimates (for the indicative depths listed in Table 2).

Consistent with the shallow nature of satellite observing depths, soil moisture estimates have been taken from the top layer of each model. Where models provide estimates at deeper defined intervals (*i.e.* WaterDyn, AWRA-L and CABLE), additional *in situ* soil moisture observations were considered to provide some assessment of how the evaluation differs when a uniform corresponding depth interval is used. Deeper *in situ* observations were available at OzNet sites NSW-01 and NSW-02 for the intervals 0–30 cm, 30–60 cm and 60–90 cm. Using a weighted arithmetic mean, a single *in situ* soil moisture time series for the depth interval 0–90 cm was calculated for both NSW-01 and NSW-02. The *in situ* measurements were then correlated with each of the WaterDyn, CABLE and AWRA-L time series based on their respective overlapping layer fractions.

3.2. Temporal anomaly

Correlation was also determined for the temporal anomalies of each data set. The performance of each product was evaluated using both the original and anomaly time series to respectively highlight agreement in soil moisture seasonality (Dorigo et al., 2015; Brocca et al., 2011; Reichle et al., 2004), as distinct from the skill of a product in detecting single events (Brocca et al., 2011).

Typically, the temporal anomaly time series is calculated using the difference between the soil moisture measurement and its long-term mean; however as the time periods covered by the different products evaluated in this study vary significantly, the soil moisture anomalies (θ_{anom}) were calculated using a 29-day moving average in the common time period (based on Albergel et al., 2009;

Table 2
Summary of comparison data sets.

	Product	Algorithm	Version	Overpass	Frequency [GHz]	Data period	Spatial resolution [km]	Depth [cm]
Satellites	SMOS	LPRM	2016	A	1.4	2010–2014	≈43	≈0–5
	SMOS	LMEB	RE04	A	1.4	2010–2014	≈43	≈0–5
	AMSR2	LPRM	1.1	D	6.9	2012–2014	≈50	≈0–2
	AMSR2	JAXA	1.1	A	10.7	2012–2014	≈50	≈0–2
	ASCAT	TUW	WARP5.5	D	5.3	2007–2013	≈25	≈0–2
Models	WaterDyn	–	26M	–	–	2001–2013	≈5	0–8 to 0–70 ^b
	CABLE	–	BIOS2	–	–	2001–2014	≈5	0–8 ^a
	AWRA-L	–	5.0	–	–	2001–2014	≈5	0–10
	API	–	–	–	–	2012–2014	≈5	Variable
	KBDI	–	–	–	–	2001–2014	≈5	Variable
	MSDI	–	–	–	–	2001–2014	≈5	Variable

^a Weighted mean of 0–2.2 cm & 2.2–8 cm intervals.

^b Typically 0–20 cm at sites considered in this study.

Kim et al., 2015). For each soil moisture measurement (either *in situ* or product) at time t (θ_t), a period of 14 days prior and 14 days after was defined. Provided at least seven measurements were available in this period, the average soil moisture ($\bar{\theta}_{anom}$) and standard deviation (σ) were calculated in order to calculate the anomaly as per Eq. (5).

$$\theta_{anom} = \frac{\theta_t - \bar{\theta}_{(t-14:t+14)}}{\sigma_{(t-14:t+14)}} \quad (5)$$

3.3. Time series visualisation

The comparison of products based on the correlation was supported by visual analysis of the soil moisture time series plots. The aim of studying the time series plots was to identify and highlight features of product temporal behaviour not apparent in the correlation analysis, lending insight to the processes driving temporal behaviour of each product across Australia.

3.4. Cluster analysis

A cluster analysis was conducted to explore the interrelationships between the products themselves. While the ability of a product to successfully reproduce *in situ* temporal behaviour was measured using R , the purpose of the cluster analysis was to show those products that closely associate with each other. Close association between products indicates similarity. Identifying similarity or lack thereof helps determine which data sets have duplicate content and may share commonalities in error structure, and which are complementary, potentially providing useful information given that multiple products are currently employed in single applications (e.g. data assimilation).

Hierarchical cluster analyses were performed at each station location to construct dendrograms where products are grouped when their degree of association is maximal. Each dendrogram is developed by ranking all possible pairs of products based on their degree of association. A hierarchy tree (dendrogram) is then created based on the ranking, beginning with the two products with the closest degree of association, all the way to the products with the least association, with the height of each link in the tree reflecting the relative degree of association between the products. The analysis was based on the Euclidean distance between product pairs of $1-R^2$ values.

3.5. Satellite overpass and frequency band selection

Prior to the product comparison, a preliminary analysis was undertaken to determine which satellite overpass (ascending or descending part of the orbit) and frequency band data sets should be used in the comparison. Fig. 2 shows the range of correlation coefficients R and standard deviation for ascending and descending passes for each of the satellite soil moisture products: SMOS_LPRM L-band, SMOS_LMEB L-band, AMSR2_LPRM C-band, AMSR2_LPRM X-band, AMSR2_JAXA X-band, and ASCAT_TUW C-band. The correlation was calculated between *in situ* and the satellite product over the longer time period of comparison and at all sites (Table 1).

Particularly interesting from Fig. 2 are the lower minimum correlations of AMSR2_LPRM C-band in the daytime overpass (ascending) compared to its night-time overpass. Data from night-time satellite overpasses are often considered more suitable for comparison with *in situ* soil moisture as night-time conditions are considered to provide better soil moisture estimates due to the increased thermal equilibrium conditions of the surface soil, canopy and near-surface air (Owe et al., 2008). The wider range of correlation for the

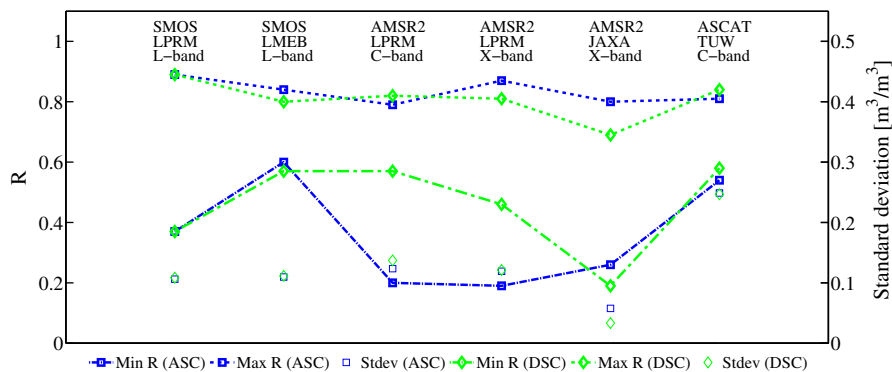


Fig. 2. Minimum and maximum coefficients of correlation between *in situ* and satellite soil moisture estimates across all stations (left axis) and standard deviation (right axis), for different satellite overpasses and frequency bands. Note the units of standard deviation for ASCAT are percentage relative wetness. ASC = ascending overpass, DSC = descending overpass.

AMSR2_LPRM C-band daytime ascending overpass is a result of a lower correlation result at the northern Australian station location NT-04 ($R = 0.20$).

Considering the night-time descending overpass, AMSR2_LPRM C-band yields a more favourable range of correlation than AMSR2_LPRM X-band. This is consistent with the expectation that X-band retrievals are more susceptible to scattering and absorption due to vegetation influences due to its shorter wavelength (De Jeu et al., 2008) and represent a shallower soil depth compared to C-band retrievals, and therefore yield poorer correlation results. Considering these factors and the difference in the range of correlation between ascending and descending for SMOS and ASCAT was less than 0.01 (Fig. 2), the night-time or early morning data sets have been selected for further analysis in this study. For the AMSR2_JAXA product, correlations were generally better under day-time ascending passes, leading to a higher correlation coefficients compared to the night-time descending data set in Fig. 2.

In summary, from this analysis the following products have been used for subsequent analysis: SMOS_LPRM_A, SMOS_LMEB_A, ASCAT_TUW_D, AMSR2_LPRM_D (C-band) and AMSR2_JAXA_A (where products are named as *satellite_algorithm_overpass*).

4. Results

4.1. Comparison of products

The comparisons in terms of the correlation coefficient (R) between *in situ* soil moisture measurements and satellite or model products are presented in Tables 3 and 5. All correlations are between the *in situ* soil moisture depth intervals listed in Table 1, and the product depth intervals listed in Table 2. Correlation coefficients are shown for both the longer period of coincident data within the study timeframe of 2001–2014 (Table 3) and common period of July 2012–July 2013 (Table 5). Values in bold indicate the highest correlation among either satellite or model products. A relative comparison of R (longer period) for each product across Australia is illustrated in Fig. 3, shown with major Köppen climate classification zones.

The results of the additional comparison between *in situ* soil moisture and modelled estimates at deeper depths are provided in Table 4 for the longer period of comparison.

Overall the satellite products yielded roughly similar ranges of correlation coefficients, with the possible exception of AMSR2_JAXA_A. The SMOS products performed slightly better than the alternative

Table 4

Summary of correlation between 0 and 90 cm *in situ* measurements and model products, longer period (2001–2014).

Station	Models		
	WaterDyn	CABLE	AWRA-L
NSW-01	0.68	0.76	0.80
NSW-02	0.66	0.72	0.66

satellite-based data sets, yielding higher correlation coefficients than the other satellite products at 11 out of 13 sites. In the longer period of comparison, SMOS_LMEB_A achieved correlation coefficients in the range 0.64–0.83 and 0.48–0.88 in the common period. SMOS_LPRM_A yielded a range between 0.37 and 0.89 in the longer period, or 0.67 and 0.89 when omitting QLD-02, where SMOS_LMEB_A returned a non-significant correlation. SMOS_LPRM_A achieved a better correlation with *in situ* measurements than SMOS_LMEB_A at over half of the locations in the longer period of comparison, and showed the highest skill among all satellite products on eight occasions compared to three occasions for SMOS_LMEB_A. However SMOS_LMEB_A returned fewer non-significant correlations than SMOS_LPRM_A in the common period owing to a comparatively larger number of data points available at each site (e.g. NT-01, QLD-01, VIC-01 and NSW-03). With the exception of QLD-02, Fig. 3 highlights that the strong, long-term agreement of the SMOS products is consistent across climate zones.

ASCAT_TUW_D and AMSR2_LPRM_D performed similarly well, with correlation coefficients in the range of 0.57–0.82 and 0.58–0.84, respectively, in the longer time period of comparison. ASCAT_TUW_D and AMSR2_LPRM_D were slightly less similar to each other in the common period of comparison, yielding a range of 0.54–0.87 and 0.39–0.89 respectively, similar to SMOS_LMEB for a comparable number of data points.

The AMSR2_JAXA_A product performed most poorly among the satellite data sets, achieving a larger range of 0.26–0.80 in the longer period, and 0.38–0.86 in the common period. Approximately half the sites yielded $R < 0.6$ in both periods of comparison. The wider range of correlation coefficients from AMSR2_JAXA_A reflects a more variable agreement across climate zones than the other satellites (Fig. 3). The higher correlation coefficients found at stations NSW-01 and NSW-02 suggest a potential calibration effect in this area, as data from this area have been used in the AMSR2_JAXA algorithm calibration process (Maeda and Taniguchi, 2013).

Table 3

Summary of correlation between *in situ* data and satellite and model products, longer period (2001–2014). Values in bold indicate the highest correlation among either satellite or model products.

Station	Satellites					Models						
	SMOS LPRM A	SMOS LMEB A	AMSR2 LPRM D	AMSR2 JAXA A	ASCAT TUW D	WaterDyn	CABLE	AWRA-L	API	KBDI	MSDI	
OzFlux	NT-01	0.74	0.68	0.65	0.52	0.63	0.79	0.81	0.77	0.79	0.45	0.58
	NT-02	0.87	0.73	0.68	0.71	0.84	0.88	0.89	0.89	0.84	0.75	0.75
	NT-03	0.77	0.65	0.78	0.77	0.81	0.83	0.82	0.79	0.84	0.72	0.71
	NT-04	0.74	0.72	0.57	0.55	0.73	0.84	0.85	0.73	0.64	0.86	0.87
	QLD-01	0.67	0.64	0.64	0.51	0.58	0.78	0.80	0.72	0.72	0.64	0.55
	VIC-01	NS	0.79	0.66	0.38	0.70	0.83	0.70	0.58	0.76	0.59	0.72
	VIC-02	0.75	0.71	0.63	0.26	0.59	0.78	0.67	0.69	0.82	0.50	0.71
OzNet	NSW-01	0.74	0.78	0.77	0.78	0.68	0.84	0.80	0.80	0.72	0.45	0.66
	NSW-02	0.78	0.81	0.80	0.80	0.69	0.83	0.80	0.80	0.77	0.42	0.68
CosmOz	NSW-03	0.85	0.81	0.82	0.67	0.83	0.87	0.77	0.61	0.71	0.63	0.84
	NSW-04	0.80	0.75	0.73	0.57	0.72	0.76	0.68	0.63	0.68	0.25	0.44
	QLD-02	0.37	NS	0.62	0.43	0.75	0.82	0.87	0.70	0.63	0.84	0.73
	QLD-03	0.89	0.83	0.75	0.63	0.84	0.88	0.89	0.77	0.82	0.73	0.77
	Range	0.37–0.89	0.64–0.83	0.57–0.82	0.26–0.80	0.58–0.84	0.76–0.88	0.67–0.89	0.58–0.89	0.63–0.84	0.25–0.86	0.44–0.87
	N (sum)	5104	6650	4861	5363	6740	16,171	17,456	17,456	10,103	17,456	17,456
	N (range)	212–590	265–716	225–612	236–681	251–896	619–2250	619–2309	619–2309	531–1096	619–2309	619–2309

NS: not significant.

Table 5
Summary of correlation between *in situ* data and satellite and model products, common period (2012–2013). Values in bold indicate the highest correlation among either satellite or model products.

	Station	Satellites					Models					
		SMOS LPRM A	SMOS LMEB A	AMSR2 LPRM D	AMSR2 JAXA A	ASCAT TUW D	WaterDyn	CABLE	AWRA-L	API	KBDI	MSDI
OzFlux	NT-01	NS	0.62	0.66	0.45	0.45	0.57	0.69	0.67	0.72	−0.15	0.31
	NT-02	0.72	0.70	0.70	0.78	0.83	0.89	0.90	0.88	0.89	0.72	0.70
	NT-03	0.81	0.69	0.78	0.77	0.89	0.90	0.90	0.81	0.88	0.86	0.82
	NT-04	0.57	0.53	0.54	0.55	0.39	0.80	0.71	0.66	0.61	0.74	0.84
	QLD-01	NS	0.48	0.63	0.45	0.41	0.63	0.64	0.58	0.58	0.70	0.52
	VIC-01	NS	0.84	0.66	0.39	0.75	0.90	0.78	0.66	0.81	0.67	0.76
	VIC-02	0.79	0.78	0.71	0.38	0.74	0.79	0.72	0.56	0.70	0.70	0.85
	OzNet	NSW-01	0.69	0.79	0.82	0.79	0.73	0.79	0.80	0.74	0.69	0.56
CosmOz	NSW-02	0.81	0.83	0.87	0.82	0.80	0.86	0.86	0.84	0.80	0.54	0.78
	NSW-03	NS	0.85	0.85	0.72	0.86	0.90	0.77	0.58	0.76	0.64	0.92
	NSW-04	0.87	0.88	0.78	0.86	0.85	0.90	0.79	0.79	0.84	0.36	0.80
	QLD-02	0.35	NS	0.57	0.40	0.78	0.85	0.85	0.64	0.69	0.83	0.73
	QLD-03	NS	0.80	0.85	0.55	0.73	0.78	0.90	0.70	0.80	0.70	0.78
	Range	0.35–0.87	0.48–0.88	0.54–0.87	0.38–0.86	0.39–0.89	0.57–0.90	0.64–0.90	0.56–0.88	0.58–0.89	−0.15–0.86	0.31–0.92
	N (sum)	1455	2147	2684	3226	2002	4696	4696	4696	4696	4696	4696
	N (range)	75–151	68–194	173–253	211–273	130–176	330–366	330–366	330–366	330–366	330–366	330–366

NS: not significant.

One difficulty in comparing time series from different satellite platforms, or different retrieval algorithms for a single platform, is the discrepancy in sampling times. The correlation results presented thus far have been based on all days within the study period where both in *in situ* time series and the product to be correlated with had finite values. Inevitably this leads to a different number of sampling points to compare (see N in Table 3 for example), as well as a difference in the timing of those points between products. Preliminary tests were carried out to provide some indication of how the correlation varies when sampling points are collocated in time between the satellite products. The agreement between a satellite product and *in situ* estimates was re-assessed using data points collocated in time between satellite product pairs.

For instance when the two SMOS products were collocated in time, the range of *R* varied little to previous estimates shown in Table 3. The correlation between SMOS_LPRM_A and *in situ* measurements ranged between 0.40 and 0.89, and SMOS_L3_A between 0.61 and 0.81. Changes at individual sites were within approximately $\pm 5\%$ of values listed in Table 3 for *N* = 6650. Similarly little change in the range of *R* was observed when the two AMSR2 products were collocated in time. AMSR2_LPRM_D ranged between 0.52 and 0.82, and AMSR2_JAXA_A between 0.26 and 0.79, for *N* = 4903.

The comparison was extended to compare *R*-values when temporally collocating products from different satellite platforms. When SMOS_L3_A and ASCAT_TUW_D were collocated in time, the correlation coefficients between SMOS_L3_A and *in situ* measurements ranged between 0.63 and 0.85. This is similar to the range previously estimated (Table 3), for a reduced number of points (*N* = 3551). ASCAT_TUW_D ranged between 0.58 and 0.84, the same range as previous (Table 3) where almost twice the number of data points were considered.

When AMSR2_LPRM_D and ASCAT_TUW_D were collocated in time, AMSR2_LPRM_D *R*-values ranged between 0.49 and 0.85. Correlation coefficients at individual sites varied approximately $\pm 10\%$, with the exception of QLD-02 (reducing from 0.62 previously to 0.50); however this was based on considerably fewer data points (*N* = 1891 compared to 4861 previously, Table 3). The range in ASCAT_TUW_D *R*-values changed little (0.45–0.89) but NT-04 saw a considerable reduction in *R*, from 0.73 (Table 3) to 0.45, again based on fewer data points.

Lastly, when SMOS_L3_A and AMSR2_LPRM_D were collocated in time, AMSR2_LPRM_D varied little from previous estimates, ranging between 0.55 and 0.82 (*N* = 3436). The correlation between SMOS_L3_A and *in situ* measurements did vary considerably at

NT-04, reducing to 0.53. Otherwise, correlation coefficients remained within approximately $\pm 10\%$ of previous estimates shown in (Table 3).

Correlation between the *in situ* measurements and modelled predictions varied between products. The WaterDyn product was the clear front runner, followed closely by CABLE. WaterDyn achieved the strongest agreement with *in situ* measurements among all the models in both the longer and common periods, and indeed was stronger than all satellite products. The higher correlation coefficients of WaterDyn compared to all satellite products was based on notably more data points (Tables 3 and 5). The correlation between WaterDyn and *in situ* measurements ranged between 0.76 and 0.88 in the longer period of comparison, and 0.57 and 0.90 in the common period. The highly consistent strength of WaterDyn across climate zones is reflected in Fig. 3. CABLE and API also performed well and were generally strong across climate zones (Fig. 3), with CABLE yielding somewhat higher correlation coefficients with *in situ* measurements than API. Despite the simplicity of API, agreement with *in situ* data was strong, ranging between 0.63 and 0.84 in the longer period and 0.58 and 0.89 in the common period. AWRA-L yielded similar ranges in both the longer and common periods of comparison (0.58–0.89 and 0.56–0.88 respectively). MSDI yielded a smaller range in correlation than KBDI in the longer period of comparison (0.44–0.87 and 0.25–0.86 respectively). In the common period the range in KBDI was wider still (−0.15–0.86), with the negative correlation value at NT-01 a result of several smaller wetting events being missed in the model output. KBDI was most variable across climate zones, displaying particular variability among the grassland stations (Fig. 3).

It is noted that the deeper and variable observation depth of the CosmOz stations was not detrimental to the correlation compared to the stations with fixed, shallower TDR and frequency-domain sensors. Significant, positive correlation coefficients were found at all CosmOz stations for all products, in both the longer and common period of comparison (with the exception of SMOS at two sites where the number of satellite data points was relatively low). This suggests that the temporal evolution of soil moisture in the deeper soil zone of CosmOz readings is similar to the shallower soil zone as estimated by the satellite and some model products, indicating hydraulic coupling of the layers.

Similarly, the strong correlation between the WaterDyn and *in situ* data sets indicates the greater depth interval of the upper WaterDyn model layer effectively simulates the temporal dynamics of the shallower surface layer measured by the *in situ* stations.

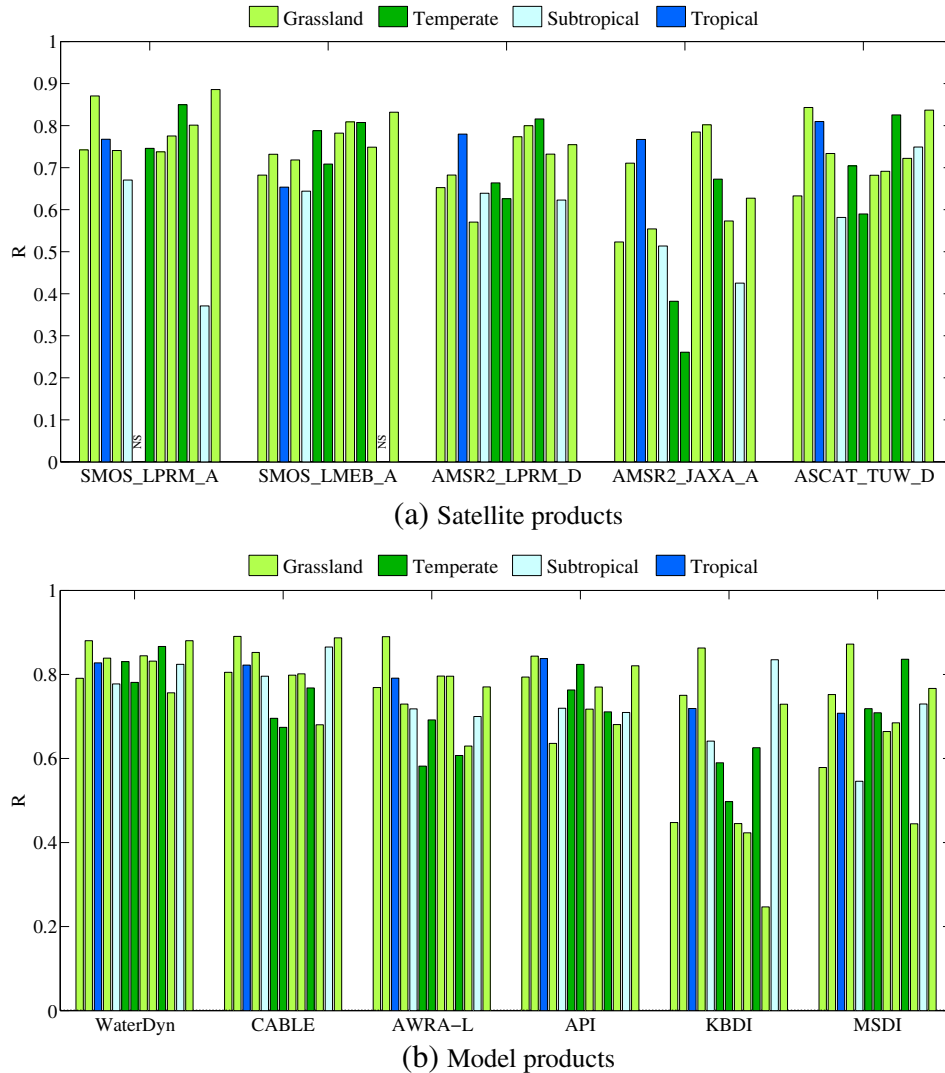


Fig. 3. Correlation across climate zones by product, longer period (2001–2014). Sites are in the same order (from top to bottom) as Table 3.

However, when looking at the results of the correlation (longer period) between OzNet measurements and each of the WaterDyn, CABLE and AWRA-L models constrained to the same depth (0–90 cm) in Table 4, correlation coefficients either remained the same or decreased. WaterDyn decreased by 0.16 and 0.17 at NSW-01 and NSW-02 respectively. AWRA-L remained the same at NSW-01 and decreased by 0.14 at NSW-02. CABLE decreased to a lesser extent, by 0.04 and 0.08 at NSW-01 and NSW-02 respectively.

4.2. Comparison of temporal anomalies

The results of the correlation between *in situ* data and satellite and model anomalies are presented in Table 6. The range of correlation coefficients between the products was similar. SMOS_LPRM_A ranged between 0.27 and 0.54, similar to SMOS_LMEB_A (0.20–0.55). A significant correlation between *in situ* measurements and SMOS estimates was not found at a number of sites, particularly SMOS_LPRM_A, due to a comparatively low number of data points; however a significant correlation was possible in many instances at a significance level of $p = 0.05$ (not shown). At sites where both products yielded a significant correlation, values were similar between products (Table 6). AMSR2_LPRM_D and AMSR2_JAXA_A yielded a

similar range of correlation coefficients, ranging between 0.20 and 0.55 and 0.24 and 0.56, respectively. ASCAT_TUW_D achieved a similar range (0.22–0.49) for relatively fewer data points.

The models showed greater skill in simulating *in situ* temporal anomalies than the satellite products. WaterDyn and CABLE continued to perform strongly relative to the other products, ranging between 0.38 and 0.77 and 0.33 and 0.78, respectively, with AWRA-L following closely with 0.34–0.76. As in the relative product comparison, the agreement of KBDI was somewhat weaker than MSDI, ranging between 0.25 and 0.70 compared to 0.29 and 0.78.

The temporal anomaly of all products showed a weaker correlation with *in situ* data than the original time series, indicating all products are more effective at detecting interannual and seasonal patterns than single events. This is likely a result of the disparity between product and *in situ* spatial support. Single events measured by *in situ* sensors represent a small point in space and thus the influence of local conditions. Even the spatial support of the CosmOz *in situ* estimates, covering approximately 30 ha surrounding the instrument, represent at best only 1.2% of the grid cell of the highest resolution products (WaterDyn, CABLE, AWRA-L, API, KBDI, MSDI) and at worst 0.05% of the lower resolution satellite products (SMOS_LPRM_A, SMOS_LMEB_A, AMSR2_LPRM_D, AMSR2_JAXA_A).

Table 6
Summary of correlation of temporal anomalies, common period. Values in bold indicate the highest correlation among either satellite or model products.

	Station	Satellites					Models					
		SMOS LPRM A	SMOS LMEB A	AMSR2 LPRM D	AMSR2 JAXA A	ASCAT TUW D	WaterDyn	CABLE	AWRA-L	API	KBDI	MSDI
OzFlux	NT-01	NS	0.40	0.39	NS	NS	0.55	0.71	0.76	0.72	0.47	0.55
	NT-02	NS	0.20	0.30	0.36	0.43	0.50	0.46	0.39	0.43	0.53	0.41
	NT-03	0.37	0.23	0.35	0.54	0.53	0.76	0.78	0.66	0.65	0.70	0.67
	NT-04	NS	NS	0.24	NS	0.22	0.57	0.38	0.45	0.38	0.57	0.53
	QLD-01	NS	0.30	0.20	0.44	NS	0.68	0.63	0.61	0.61	0.48	0.60
	VIC-01	NS	0.34	0.32	0.36	NS	0.77	0.67	0.59	0.65	0.70	0.78
	VIC-02	NS	NS	0.22	0.24	NS	0.47	0.33	0.34	0.40	0.40	0.40
OzNet	NSW-01	0.38	0.34	0.46	0.38	0.30	0.52	0.51	0.52	0.51	0.38	0.41
	NSW-02	0.54	0.55	0.52	0.56	0.26	0.67	0.69	0.68	0.65	0.48	0.57
CosmOz	NSW-03	NS	0.33	0.48	0.27	0.33	0.58	0.59	0.55	0.62	0.32	0.51
	NSW-04	0.27	0.22	0.39	0.30	0.30	0.38	0.37	0.37	0.37	0.25	0.29
	QLD-02	NS	NS	NS	NS	0.44	0.47	0.49	0.47	0.48	0.43	0.35
	QLD-03	NS	0.39	0.55	0.39	0.49	0.50	0.56	0.46	0.51	0.44	0.50
	Range	0.27–0.54	0.20–0.55	0.20–0.55	0.24–0.56	0.22–0.49	0.38–0.77	0.33–0.78	0.34–0.76	0.37–0.72	0.25–0.70	0.29–0.78
	N (sum)	1455	1999	2721	3003	1859	4354	4354	4354	4354	4354	4354
	N (range)	75–151	64–178	158–235	202–254	125–164	317–337	317–337	317–337	317–337	317–337	317–337

NS: Not significant.

At the larger product scales soil moisture dynamics are more likely to be influenced by broad atmospheric controls (Brocca et al., 2014).

4.3. Time series visualisation

Visual inspection of the time series at each station location provided further insight into the differences in agreement of satellite and model soil moisture products with *in situ* measurements. The purpose of this section is to summarise the main features of interest within the time series to complement the findings of the correlation analysis.

The SMOS_LPRM_A and SMOS_LMEB_A products were shown to yield slightly higher correlation coefficients than other satellite products in the correlation analysis overall. This was reflected in the time series plots, where both products had a good visual fit to the *in situ* data. An example plot is shown in Fig. 4 at station NSW-03. Seasonal and annual cycles had a better visual fit to the *in situ* data than shorter term dynamics, particularly at the drier northern locations. Both SMOS products displayed a reduced sensitivity to soil moisture change during dry periods (e.g. soil moisture < 0.1 m³/m³), especially at the drier sites of the Northern Territory. It is noted that SMOS_LMEB_A often showed contrary short-term temporal behaviour to SMOS_LPRM_A during the periods of reduced sensitivity. The two AMSR2 soil moisture products were not as similar

as the two SMOS products. AMSR2_LPRM_D showed a tendency to dry down more slowly than *in situ*, displaying a more concave drying process. This behaviour was evident at all stations to some extent, but was most apparent at the end of the wet season at the drier Northern Territory locations, reflected in their lower correlation values there. An example of this effect is shown for NT-01 in Fig. 5. This effect was not observed in the AMSR2_JAXA_A time series. At some south-eastern Australian stations the winter wet period was on one occasion lagged by several months in the AMSR2_JAXA_A time series (NSW-04) or missed entirely (VIC-01 and VIC-02), resulting in a poorer correlation at these locations compared to the other satellite products (Table 3).

Similar to the other satellite products, the ASCAT_TUW_D product had a good visual fit to the *in situ* data, more so at annual and seasonal scales than for short-term dynamics. The time series of the ASCAT_TUW_D product was smoother than *in situ* at the drier, northern Australia stations, particularly those characterised by open wooded vegetation (e.g. NT-02, illustrated in Fig. 6).

Analysis of the WaterDyn, CABLE and API time series consistently showed a good visual temporal fit to *in situ* data across station locations (e.g. Fig. 7).

Analysis of the KBDI product time series showed a tendency to dry too slowly after wet periods and individual rainfall events (e.g. Fig. 8). The visual fit of the time series to *in situ* was generally better at the northern and eastern Australian locations. Long-term soil moisture

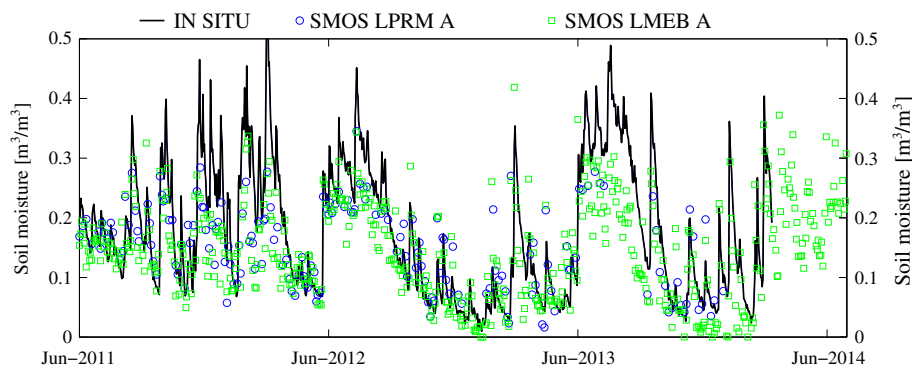


Fig. 4. SMOS_LPRM_A and SMOS_LMEB_A at NSW-03 (CosmOz network). *In situ* time series on left axes; product time series on right axes.

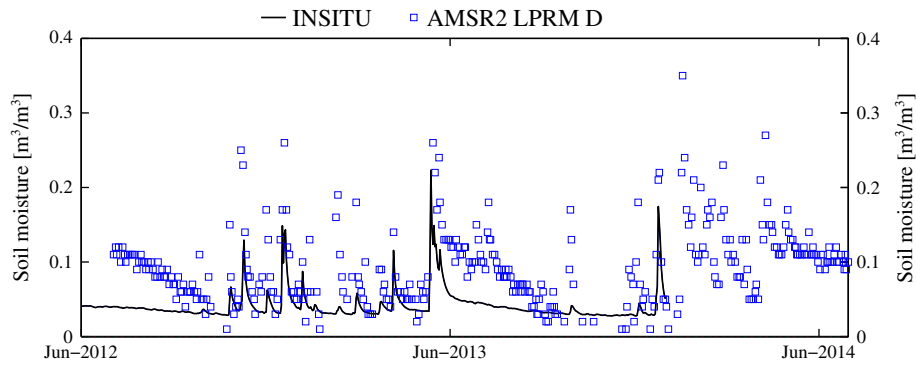


Fig. 5. AMSR2_LPRM_D at NT-01 (OzFlux network). *In situ* time series on left axes; product time series on right axes.

dynamics were not represented well at most stations in the south-east, as reflected in Fig. 3.

MSDI showed similar characteristics to KBDI in the time series plots. Dry down dynamics were also slow compared to the *in situ*, but to a lesser extent than KBDI at all sites and therefore MSDI achieved more favourable correlation values in both the longer and common periods of comparison.

Unlike the KBDI product, the AWRA-L time series occasionally showed a tendency to dry down too quickly compared to *in situ* measurements (Fig. 8). While this observation was evident at all stations, it was most prominent at the northern Australian locations where *in situ* measurements showed a prolonged period of decreasing soil moisture following the wet season. Nonetheless the overall wet/dry seasonal patterns were reflected well in the AWRA-L time series.

The short-term variability in *in situ* anomalies was noticeably larger at locations where cosmic-ray instruments were used. Soil moisture measurements from cosmic-ray sensors are subject to correction procedures, the largest of which relates to changes in atmospheric pressure (Hawdon et al., 2014), and may account for the increased short-term variability. This pattern of higher short-term variability at cosmic-ray sites compared to TDR and frequency-domain sensor sites in a similar location was also visible in the time series of absolute soil moisture values, but with more pronounced differences in correlation between products in the anomaly time series.

4.4. Cluster analysis

The cluster analysis was based on a matrix of $1-R^2$ values, with the aim of highlighting products that closely associate with each other.

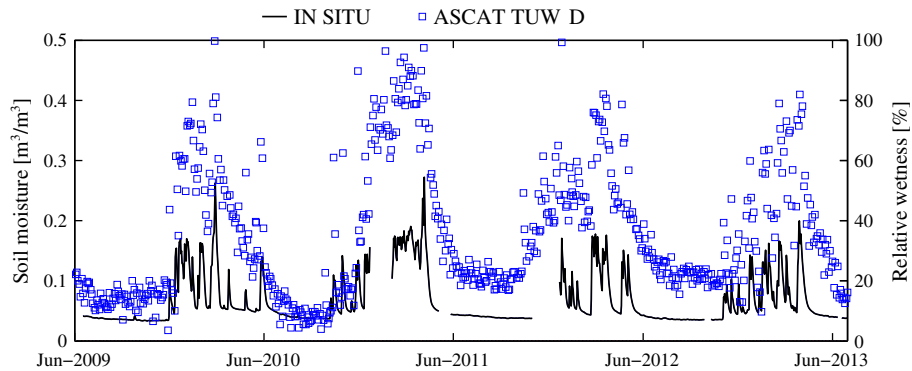


Fig. 6. ASCAT_TUV_D at NT-02 (OzFlux network). *In situ* time series on left axes; product time series on right axes.

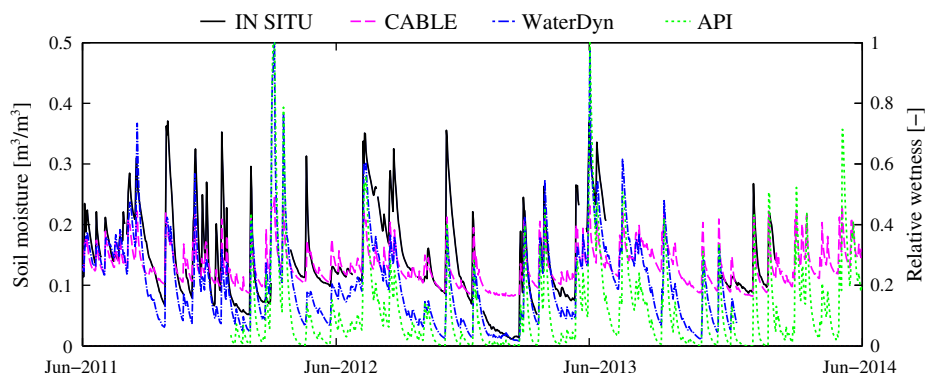


Fig. 7. CABLE, WaterDyn and API at NSW-02 (OzNet network). *In situ* and CABLE time series on left axes; WaterDyn and API time series on right axes.

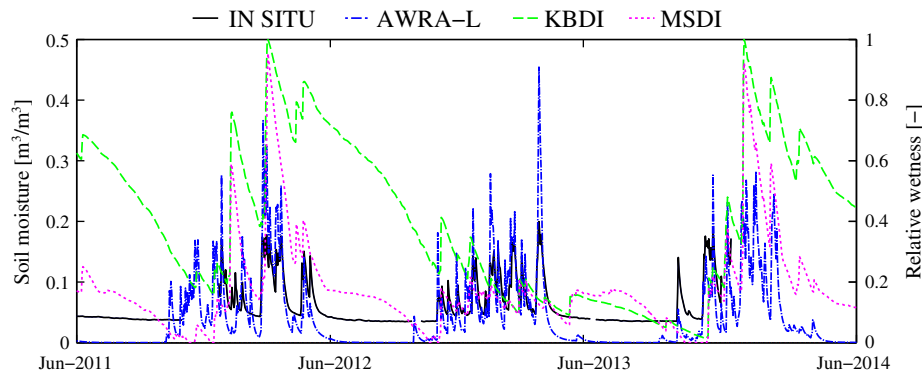


Fig. 8. AWRA-L (0–10 cm), KBDI and MSDI at NT-01 (OzFlux network). *In situ* time series on left axes; product time series on right axes.

Products that group together may indicate similarities in their error structure. Grouping is expected given that dependence exists among some products (e.g. model products use the same AWAP forcing data and both SMOS products use the same input brightness temperature data, as do the AMSR2 products).

A cluster analysis was carried out for each station location. The 1- R^2 matrices included all products (and *in situ* estimates) with the exception of SMOS_LPRM_A, which could not be correlated with some products due to a lack of coincident data, and so could not be included in the clustering matrices. Furthermore a cluster analysis could not be performed at QLD-02 due to a lack of significant correlation between SMOS_LMEB_A and other products at the $p = 0.01$ level. The hierarchical cluster dendrograms are provided in the Appendix for the longer period of comparison.

In general, satellite products clustered with other satellite products, and model products with model products, this being clearest at grassland climate zone locations NT-01, NT-04, NSW-01, NSW-02 and NSW-04, and temperate zone location VIC-02. At the remaining sites, the satellite/satellite and model/model groupings were less evident, often due to ASCAT_TUW_D, AMSR2_LPRM_D or AMSR2_JAXA_A grouping with one or more of the model products. Interestingly, SMOS_LMEB_A and ASCAT_TUW_D grouped at eight out of the 12 locations; however, no clear patterns between climate zones or vegetation types/density were apparent. As expected, KBDI and MSDI showed a close association and paired at all but one site. The WaterDyn, CABLE, AWRA-L and API products grouped together at most locations, with AWRA-L grouping with API at nine locations. WaterDyn and CABLE paired closely, particularly at the NT grassland zone stations. AMSR2_LPRM_D and AMSR2_JAXA_A did not group (i.e. were different to each other) at 10 out of 12 sites. *In situ* measurements grouped closely with models at nine out of 12 sites, but did not show a preference for a particular model product.

It is noted that filtering of the product time series, or analysis of the time series on a longer time scale (e.g. monthly), may potentially bring out similarities not observed here. Strong variability in the soil moisture record is present at daily time scales. On a daily time scale, there is a mismatch of sampling times between satellites and *in situ* measurements, and often models are forced with inexact timing of precipitation events (Reichle et al., 2004).

5. Discussion

5.1. Comparison with previous studies

The results of the correlation analysis are comparable to other studies, which mainly focus on the OzNet *in situ* network in

south-eastern Australia. For example Van der Schalie et al. (2015) compared SMOS_LPRM (ascending) to OzNet sites NSW-01 and NSW-02 for the period 2010–2011. The LPRM was run for the SMOS data set using two alternative sources of effective soil temperature input data and several incidence angles. Their study estimated correlation coefficients at sites NSW-01 and NSW-02 (on average for all incidence angles and input sources) of 0.75 and 0.88, respectively. This compared well to the findings in this study ($R = 0.74$ and $R = 0.69$ in the longer and common periods at NSW-01, and $R = 0.78$ and 0.81 at NSW-02; Tables 3 and 5). Van der Schalie et al. (2015) also compared *in situ* data to the SMOS_LMEB product, and estimated very similar correlation coefficients to SMOS_LPRM.

Su et al. (2013) also compared OzNet *in situ* data to satellite products, including ASCAT_TUW and SMOS_LMEB, for the period 2001–2012. Average correlation between all sites and ASCAT_TUW was estimated to be 0.67 (descending overpass), similar to that found in this study for the period 2001–2014 (range of 0.68–0.72 of stations NSW-01, NSW-02 and NSW-04; Table 3). The association between SMOS_LMEB and *in situ* was weaker in the previous study ($R = 0.71$ compared to 0.78–0.81 here, ascending overpass) noting that the 2013 study used an earlier version of the SMOS_LMEB product.

Frost et al. (2015) compared monthly 0–5 cm *in situ* surface soil moisture measurements from 38 sites in the OzNet network (December 2001–May 2012) to estimates derived from CABLE, WaterDyn and AWRA-L models, as well as ASCAT_TUW. CABLE and WaterDyn were found to perform more strongly than AWRA-L and ASCAT_TUW_D at OzNet sites, consistent with the findings in this study. Furthermore, Frost et al. (2015) found that CABLE and AWRA-L were better than WaterDyn when compared to deeper profile (0–90 cm) *in situ* measurements, a result reflected in this study.

Lastly, Kumar et al. (in press) compared KBDI and MSDI estimates with OzNet data for the period September 2009 to May 2011. Kumar et al. (in press) reported the average correlation between the 0–30 cm *in situ* measurements and KBDI as 0.60, and 0.71 for MSDI. These values are higher than those found in this study between the 0–10 cm *in situ* measurements and KBDI (0.45 and 0.42 at NSW-01 and NSW-02 respectively) and MSDI (0.66 and 0.68 at NSW-01 and NSW-02 respectively).

5.2. Satellite performance

The range of agreement with *in situ* estimates was similar among the satellite products, with the exception of AMSR2_JAXA_A. SMOS_LPRM_A and SMOS_LMEB_A showed a closer association to *in situ* estimates at most sites compared to other satellite products. Both SMOS products better reflected annual and seasonal variation

than short-term events. The process driving the strength of the SMOS L-band instrument is the estimation of soil moisture at a greater observation depth than the other satellites, which utilise the shorter wavelengths of the C- and X-bands. The longer wavelength of the L-band instrument is also beneficial in that it is less influenced by cloud and vegetation cover (De Jeu et al., 2008). These benefits are consistent with the findings of this study, where close association with *in situ* data was found consistently across station locations with different soil and vegetation characteristics and climate zones with the exception of QLD-02, a site located within dense tropical vegetation. At this site both SMOS products showed limited agreement with *in situ* measurements, corresponding to the known limitation of the LPRM over densely forested areas (Van der Schalie et al., 2016). At this particular site, ASCAT_TUW_D was better able to reflect *in situ* temporal dynamics than SMOS. Furthermore, both SMOS products displayed a reduced sensitivity to soil moisture change during dry periods, especially at the drier sites of the Northern Territory. This is in line with De Jeu et al. (2008), where it was shown that the dielectric constant has a reduced sensitivity to changes in soil moisture under dry conditions.

AMSR2_LPRM (C-band) exhibited clear differences in correspondence with *in situ* measurements during the daytime (ascending) and night-time (descending) parts of the orbit (Fig. 2). The process driving this finding is likely in part the differing of canopy and surface soil temperatures from the assumption of equality in the LPRM method. More intense heating of the ground surface in the daytime is noted by Owe et al. (2008) as being a significant problem for arid, semi-arid and possibly temperate regions as well, especially in areas with a high proportion of bare soil, a common feature across much of Australia. The estimation of effective temperature is an area of ongoing improvement in the LPRM development. Furthermore, vegetation density may also be affecting the difference in daytime ascending and night-time descending overpass retrievals, especially at the tropical rainforest site QLD-02. Lei et al. (2015) show that in the United States the relative advantage of night-time retrievals (of AMSR-E, predecessor of AMSR2) degraded over more heavily vegetated areas, and may help explain this result.

The AMSR2_LPRM_D product showed a moderately close association with *in situ* data overall, yet displayed slower dry down behaviour particularly within the grassland and tropical locations of the Northern Territory. The process driving this observation may be the greater influence of vegetation on the brightness temperatures in the C-band, causing the area of the satellite footprint to appear wetter for longer at the end of wet periods than in the deeper penetrating L-band. For example where *in situ* sensors are located in an area of bare soil or grass within a woodland or savannah, the soil moisture as recorded by the sensor would *a priori* be expected to rise and fall more rapidly compared to a smoother signal from the taller, more established vegetation within the satellite footprint. The smoother soil moisture signal of the satellite product is matched by the vegetation optical depth signal, sourced in parallel with AMSR2 C-band soil moisture retrievals.

While the dry down processes observed in the ASCAT_TUW_D time series better matched *in situ* data than AMSR2_LPRM_D, it showed a similarly smooth signal at some locations. However, a strength of ASCAT_TUW is the ability to separate backscatter due to soil moisture and vegetation. The soil moisture data set may be improved in future through the inclusion of dynamic vegetation correction (Vreugdenhil et al., 2016).

Moreover, the success of ASCAT_TUW_D in reflecting *in situ* temporal dynamics at a site of dense tropical vegetation (QLD-02) compared to the SMOS and AMSR2 products may be indicative of a potential relative product strength. This is in line with previous studies that compared soil moisture estimates retrieved from ASCAT with those retrieved from passive microwave sensors (e.g. Al-Yaari et al., 2014).

AMSR2_JAXA_A performed most poorly among the satellite products in terms of correlation of relative soil moisture values. The assumption in the JAXA algorithm of a constant surface and canopy temperature of 295 K ($\approx 22^\circ\text{C}$) at all locations and times is not reflective of the range of Australian conditions (e.g. see mean annual temperature ranges of sites in Table 1), and may represent an important weakness of this product over Australia.

Tests carried out to assess how the correlation varied when different satellite product pairs were colocated in time showed differences of approximately 5–10% compared to the correlation based on all coincident satellite and *in situ* finite values. Considerable differences were observed at site NT-04 (in the SMOS_L3_A data set when colocated with AMSR2_LPRM_D), suggesting the agreement between *in situ* and remotely sensed soil moisture may be more sensitive at this site than at others considered. This is reasonable given that NT-04 is located within a grassy plain in northern Australia where soil moisture is typically quite variable. However, it should be kept in mind that the change in correlation at these two sites when satellite pairs were colocated in time was based on fewer data points than when all coincident satellite and *in situ* points were considered.

5.3. Model performance

In the correlation analysis the WaterDyn product had the strongest agreement with *in situ* measurements across all products considered in this study, and most consistently across locations in different climate zones and with different soil and vegetation characteristics. The calculation of the upper soil layer water mass balance and subsequent conversion to relative soil moisture proved to effectively simulate soil moisture temporal dynamics as measured by the *in situ* sensors. CABLE was similarly able to reproduce *in situ* temporal dynamics, but was less consistent across climate zones (particularly at the temperate locations) compared to WaterDyn.

The API data set was found to be quite successful in simulating annual and seasonal dynamics of soil moisture across all station locations and climate zones considered in this study. The variation in performance across locations may be indicative of variation in the rainfall input data quality, and would need to be further tested, including an inspection of gauge inputs to the gridded data. The success is particularly compelling given the simplified nature of the index, based only on rainfall and temperature data inputs. The simplicity of the API index is considered a strength of this product. However API does not consider ecohydrological processes and energy fluxes. Instead, these are strengths of the AWRA-L model, which is process-based and includes sub-routines for water and energy fluxes, allowing vegetation to adjust accordingly.

Although the AWRA-L product correlated well with shallow *in situ* measurements at most locations, AWRA-L showed poorer agreement than API at seven locations (longer period). While no clear geographical or climatic pattern was discernible in the AWRA-L correlation results, it is possible that the association was affected by the calibration of the model to streamflow observations. When comparing deeper (0–90 cm) soil moisture measurements and AWRA-L, the correlation remained the same at one site (NSW-01) and reduced at another (NSW-02). Frost et al. (2015) undertook a more comprehensive assessment of deeper (0–90 cm) soil moisture measurements with AWRA-L in south-east Australia (at over 30 sites) and found correlation coefficients in the order $0.7 < R < 0.8$, indicating AWRA-L may be able to effectively simulate both surface and root-zone soil moisture in this area. Frost et al. (2015) found CABLE to perform similarly to AWRA-L in the deeper profile in this area, and WaterDyn slightly worse.

The weaker agreement of KBDI reflected the poor simulation of drying processes observed in the *in situ* measurements. In terms of mimicking *in situ* soil moisture temporal behaviour, the processes

driving the weakness of KBDI were two-fold. Firstly, ET is a function of vegetation cover in the KBDI model, which is itself a function of mean annual rainfall. It does not consider other factors affecting the likelihood of the vegetation being present such as soil type or latitude (Keetch and Byram, 1968). Moreover, modelled ET was only controlled by rainfall and temperature (and the previous day's soil moisture condition), without consideration of other meteorological factors such as net radiation, wind speed, or relative humidity. Secondly, the KBDI model is simplified and does not consider additional processes such as deep drainage or spatiotemporal changes to infiltration. Overall, KBDI displayed the greatest variability in performance across the sites, showing particular variability among the locations in the grassland climate zone.

While the MSDI model is similar to KBDI, its relative strength lies in the different simulation of rainfall-runoff and ET. In KBDI rainfall infiltrating the soil is lessened by a constant 5 mm of the first part of the event, regardless of vegetation cover or how the loss is partitioned between canopy interception and runoff (Finkele et al., 2006). MSDI treats them separately, and varies them depending on vegetation cover. Each grid cell is assigned one of seven vegetation classes, each with their own values of canopy interception, canopy storage and wet evaporation rates (Finkele et al., 2006). While the estimation of ET in the MSDI model is slightly more comprehensive than in KBDI, a weakness of MSDI is that it uses linear relationships between monthly pan evaporation and monthly maximum temperatures from capital cities in the south-east of Australia only, and yet is applied nation-wide across all climate zones (Kumar et al. in press; Finkele et al., 2006). Lastly, evaporation is again only a function of rainfall and temperature, and vegetation cannot adjust based on water or energy availability as it can in AWRA-L.

Although the model products achieved stronger coefficients of correlation than the satellite products in many instances, it should be noted that the strength of the model products may be in part due to their higher resolution (Table 2). Despite the model products showing stronger agreement with *in situ* measurements than the satellite products in many instances, this was not always the case, and may be partially attributed to the greater number of data points used in the correlation between model and *in situ* estimates (Tables 3 and 5), as well as to the differences in methodological approach.

5.4. Interrelationships between products

The results of the cluster analysis showed some grouping of products. Generally satellite products grouped with other satellite products, and model products with other model products, indicating potential duplication of information and potential similarities in error structures between satellite-satellite and model-model groups. However the general distinction between satellite and model products from each other indicates complementarity may exist between the data sets. Both have implications for applications utilising multiple products such as land surface model data assimilation.

It may be expected that products sharing commonalities in their approach (e.g. models share AWAP forcing data; some satellites share the same microwave sensing frequency) would cluster closely together. However, despite general grouping of satellite products with other satellites and models with models, this was not always the case. For instance, the lack of grouping between the AMSR2 products at most sites highlights the dissimilar nature of these soil moisture estimates, despite their common brightness temperatures, indicating a potential lack of commonality in their error structures and potential complementarity.

On the other hand, despite their very different approaches, the strong intercorrelation ($R > 0.85$) and close grouping of API and AWRA-L in the cluster analyses indicates that the net effect of precipitation infiltration, soil evaporation and drainage of the top soil layer

in the AWRA-L model produces very similar temporal behaviour to the API model, driven only by precipitation and temperature.

WaterDyn and CABLE intercorrelated strongly in the cluster analyses ($R > 0.75$) and particularly at the Northern Territory sites ($R > 0.94$). The two models also yielded similarly strong correlation coefficients with *in situ* at the Northern Territory sites, particularly in the longer period (both $R > 0.79$). This indicates that the models are most similar in their ability to successfully reproduce *in situ* temporal dynamics, and suggests that their model approaches are most similar to each other, at these sites.

Moreover, KBDI and MSDI paired closely, intercorrelating very strongly (range: 0.73–0.99) across the sites. This result confirms the similarity in the index model approaches, and indicates potential similarity in error structure.

Lastly, the tendency of SMOS_LMEB_A and ASCAT_TUW_D to cluster together at most locations reflects their strong temporal intercorrelation (range: 0.64–0.87) despite their differing sensors, algorithms and observation depths. That there was no clear pattern between climate zones and vegetation type/density from the clustering suggests other factors may be influencing the strong similarity in temporal soil moisture dynamics between SMOS_LMEB_A and ASCAT_TUW_D. Future clustering with SMOS_LPRM_A may help distinguish whether the similarity is algorithm-based, or more attributable to instrument features such as spatial resolution, microwave frequency and observation depth, or other factors.

6. Conclusions

This study sought to compare a wide range of sources of surface soil moisture information in a common framework, to understand how their relative performance varies across Australia and how products interrelate. To this end, 11 sources of soil moisture data were evaluated; five satellite and six model products, plus *in situ* data from three separate networks across the country. The Pearson correlation coefficient was used as the primary statistical metric to evaluate the relative temporal fit between satellite and model data sets with *in situ* measurements, which served as a reference.

The comparison of the products, as measured by their correlation with *in situ* estimates, varied between products and locations around Australia. The satellite products displayed an overall similar level of temporal association with *in situ* measurements, with the possible exception of AMSR2_JAXA_A. The two SMOS products showed the closest association with *in situ* estimates at most sites across the climate zones, owing to the deeper observation depth of the L-band sensor, with the exception of one site located in an area of dense tropical vegetation.

The AMSR2_LPRM_D and ASCAT_TUW_D products showed slower dry down behaviour than *in situ* measurements, likely a result of the greater influence of vegetation on the brightness temperatures in the C-band. The poorer temporal association of AMSR2_JAXA_A with *in situ* compared to the other satellite products may be due to the assumption in the retrieval algorithm of a constant surface and canopy temperature at all locations and times, and assumption not reflective of the range of Australian conditions.

The WaterDyn model, followed closely by CABLE, showed the closest association with *in situ* estimates out of the model products. API and AWRA-L also yielded strong agreement with *in situ* estimates.

API highlights how a simplified measure can in this case prove to be almost as successful as comprehensive process-based models in simulating temporal surface soil moisture dynamics on a daily basis. API is an index used as a proxy for soil moisture, and is a function of rainfall and temperature only. The variation in performance across sites may be indicative of variation in quality of the input data, particularly rainfall, and requires further examination. The utility

of satellite-based rainfall may also be considered, and may prove particularly useful in gauge-sparse areas.

KBDI displayed slower dry down behaviour compared to *in situ* measurements and had the highest variability across sites and climate zones of all products. The related index, MSDI, was slightly more successful at reproducing *in situ* temporal dynamics but showed poorer consistency than the strongest performing models.

The comparison of products may differ when considering different temporal and spatial scales, and it is recommended that future work consider this where commensurate with product application. All products were better able to reflect the interannual and seasonal temporal behaviour of the *in situ* reference than short-term dynamics, as reflected in the poorer temporal anomaly correlation results.

In situ soil moisture data sourced from cosmic-ray sensors were evaluated alongside soil moisture data collected from more traditional TDR and frequency-domain sensors. Cosmic-ray sensors vary in effective depth dependent on soil moisture, as satellite observations do. Future research may consider investigating the difference in correlation between satellite remotely sensed estimates and cosmic-ray sensors and their TDR counterparts, where both sets of *in situ* data are available at the same station location.

Clustering analysis revealed a general grouping of satellite products with other satellite products, and model products with model products. The general distinction between model and satellite products indicated potential complementarity between the data sources, whereas clustering of product pairs within the model and satellite

categories suggested potential similarities in error structure and duplicate information may exist between products.

Acknowledgements

This research was undertaken as part of the Australian Energy and Water Exchange research initiative (OzEWEX) Soil Water Estimation and Evaluation Project (SWEEP) whose aim is to evaluate soil moisture products against *in situ* observations across a variety of landscapes in order to identify when and where certain products are better than others (for more information visit www.ozewex.org).

The authors thank all those involved in the provision of soil moisture data, including: the CSIRO funded CosmOz network (cosmoz.csiro.au) and Aaron Hawdon for provision of data; the University of Melbourne and Monash University for provision of data and Xiaoling Wu, Alessandra Monerris-Belda, Frank Winston and Rodger Yound for data processing and network maintenance of the OzNet network; TU Wien for the production of the ASCAT data set; the Japan Aerospace Exploration Agency for the provision of the AMSR2_JAXA data set; the Centre Aval de Traitement des Données in France for the provision of the SMOS_LMEB data set. Vanessa Haverd, Cathy Trudinger and Peter Briggs thank the support of the Australian Climate Change Science Program. The contribution of Richard De Jeu and Robin Van Der Schalie was funded by the European Space Agency through the Climate Change Initiative for Soil Moisture (Contract 4000104814/11/I-NB). Finally, the authors wish to thank the three anonymous reviewers whose comments and suggestions helped improve the paper.

Appendix: cluster dendrograms by station

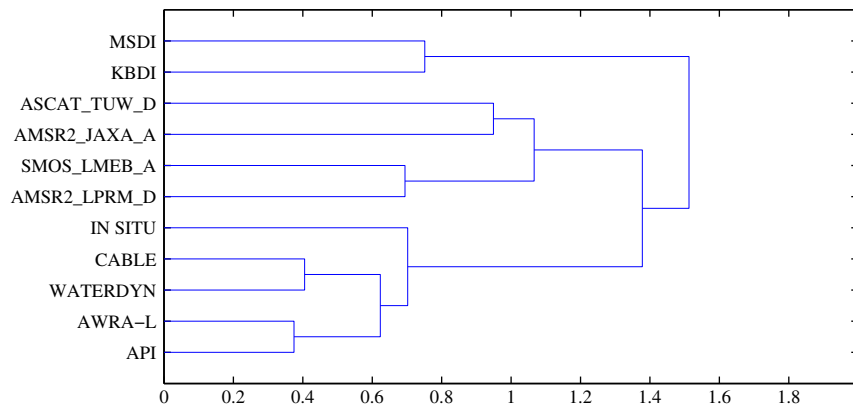


Fig. A1. NT-01.

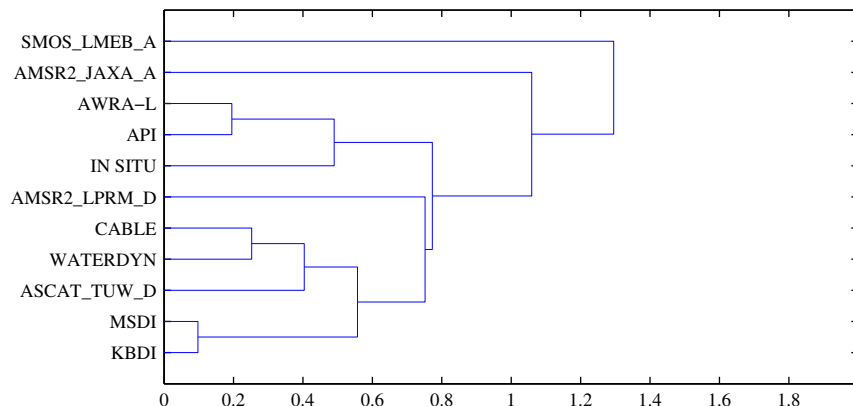


Fig. A2. NT-02.

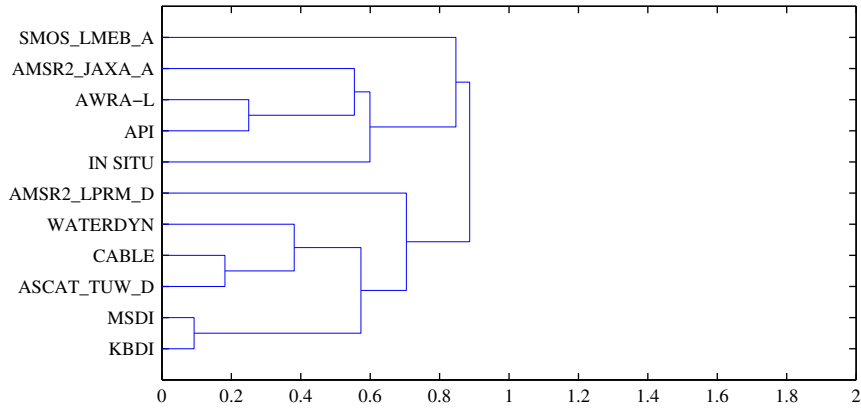


Fig. A3. NT-03.

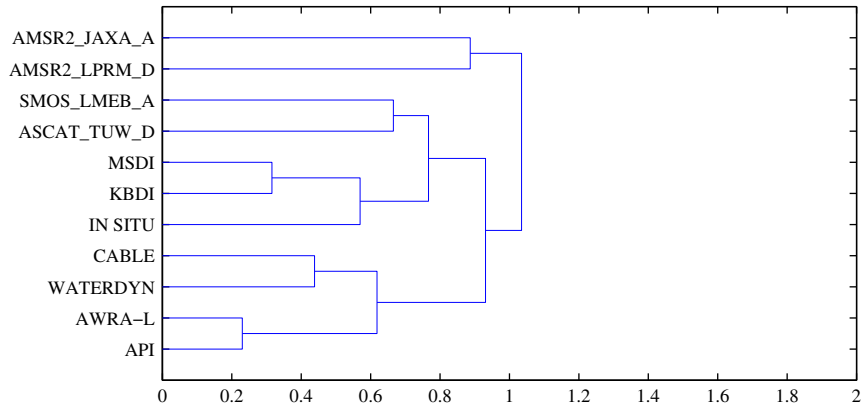


Fig. A4. NT-04.

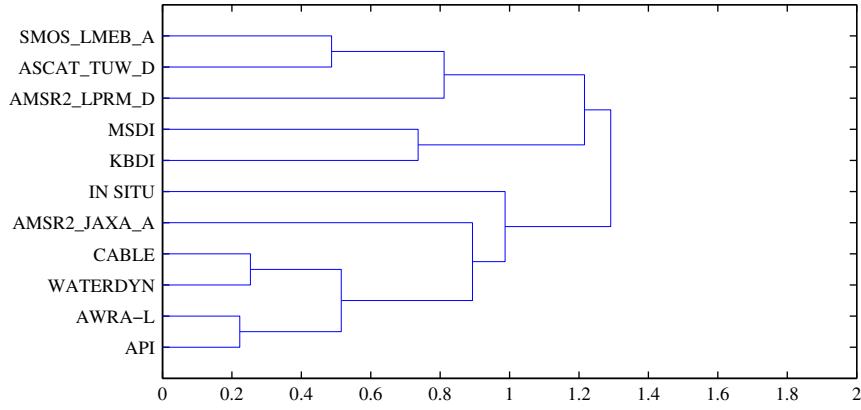


Fig. A5. QLD-01.

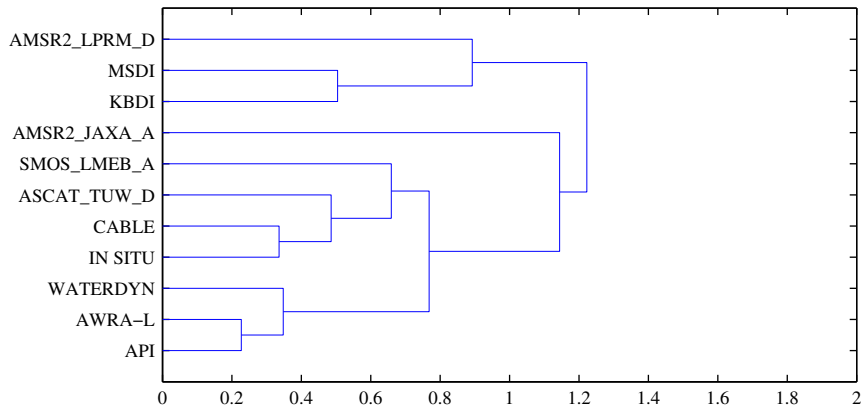


Fig. A6. QLD-03.

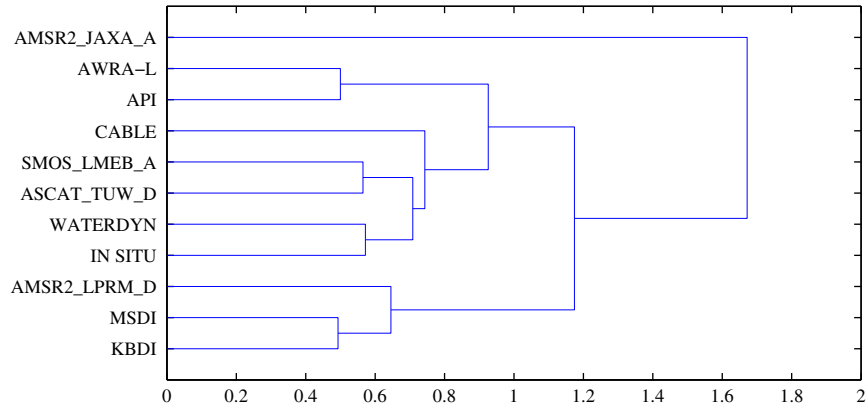


Fig. A7. VIC-01.

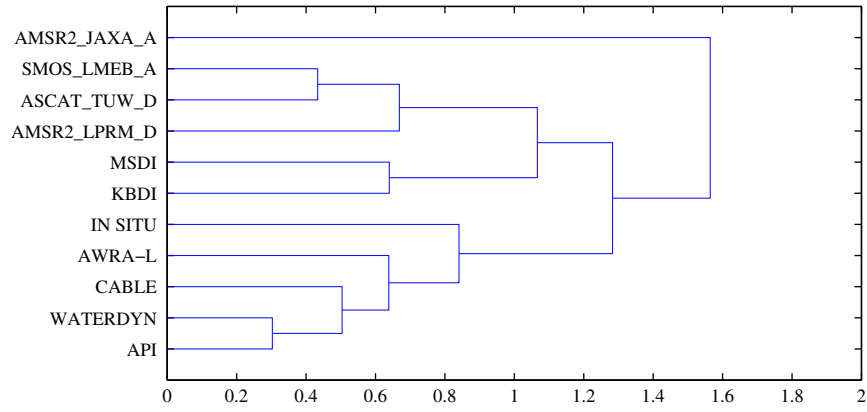


Fig. A8. VIC-02.

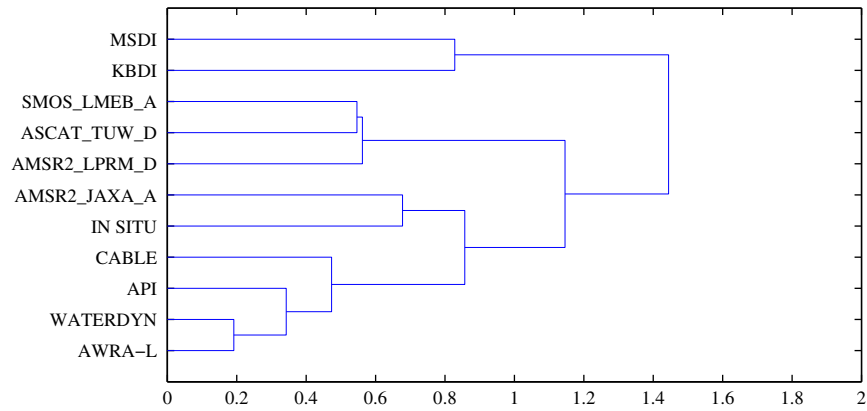


Fig. A9. NSW-01.

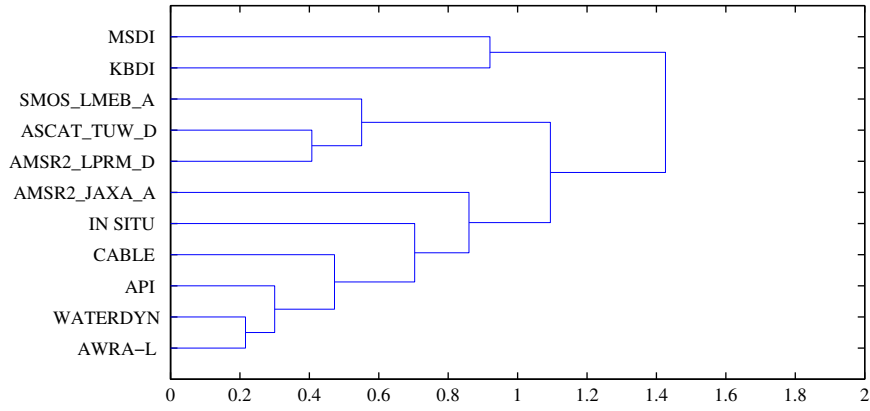


Fig. A10. NSW-02.

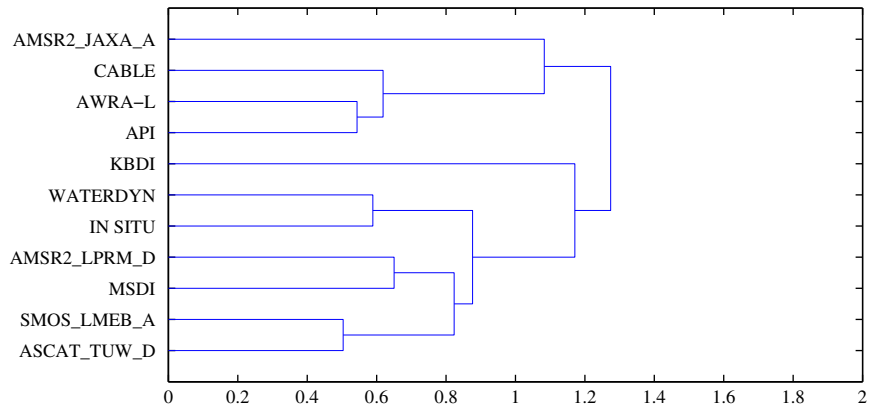


Fig. A11. NSW-03.

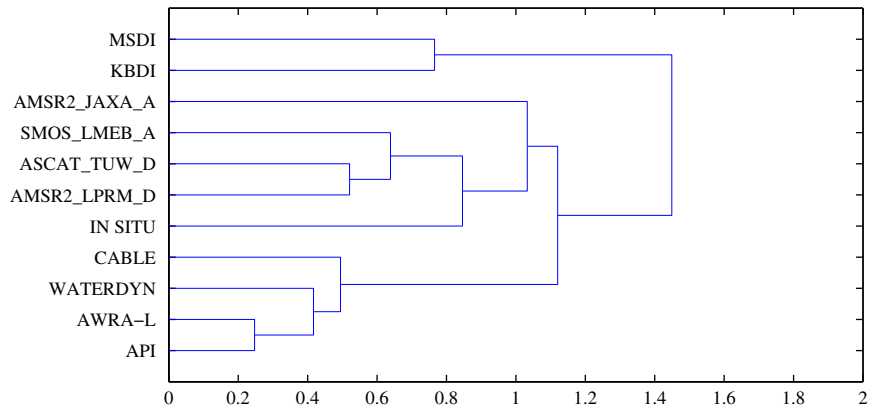


Fig. A12. NSW-04.

References

- Albergel, C., de Rosnay, P., Gruhier, C., Munoz-Sabater, J., Hasenauer, S., Isaksen, I., Kerr, Y., Wagner, W., 2012. Evaluation of remotely sensed and modelled soil moisture products using global ground-based in situ observations. *Remote Sens. Environ.* 118, 215–226.
- Albergel, C., Rüdiger, C., Carrer, D., Calvet, J.C., Fritz, N., Naeimi, V., Bartalis, Z., Hasenauer, S., 2009. An evaluation of ASCAT surface soil moisture products with in-situ observations in southwestern France. *Hydrol. Earth Syst. Sci.* 13, 115–124.
- Al-Yaari, A., Wigernon, J.P., Ducharme, A., Kerr, Y.H., Wagner, W., De Lannoy, G., Reichle, R., Al Bitar, A., Dorigo, W., Richaume, P., Mialon, A., 2014. Global-scale comparison of passive (SMOS) and active (ASCAT) satellite based microwave soil moisture retrievals with soil moisture simulations (MERRA-land). *Remote Sens. Environ.* 152, 614–626.
- Baldocchi, D., 2008. Breathing of the terrestrial biosphere: lessons learned from a global network of carbon dioxide flux measurement systems. *Australian J. Botany* 56, 1–26.
- Beringer, J., 2013. Dry River Ozflux Tower Site Ozflux: Australian and New Zealand Flux Research and Monitoring Hdl: 102.100.100/ 14229.
- Beringer, J., 2013a. Sturt Plains Ozflux Tower Site Ozflux: Australian and New Zealand Flux Research and Monitoring Hdl: 102.100.100/ 14230.
- Beringer, J., 2013b. Whroo Ozflux Tower Site Ozflux: Australian and New Zealand Flux Research and Monitoring Hdl: 102.100.100/ 14232.
- Beringer, J., 2014. Red Dirt Melon Farm Ozflux Tower Site Ozflux: Australian and New Zealand Flux Research and Monitoring Hdl: 102.100.100/ 14245.
- Beringer, J., 2014a. Riggs Creek Ozflux Tower Site Ozflux: Australian and New Zealand Flux Research and Monitoring Hdl: 102.100.100/ 14246.
- Briggs, P.R., 2016. Personal Communications.
- Brocca, L., Zucco, G., Mittelbach, H., Moramarco, T., Seneviratne, S.I., 2014. Absolute versus temporal anomaly and percent of saturation soil moisture spatial variability for six networks worldwide. *Water Resour. Res.* 50, 5560–5576.
- Brocca, L., Hasenauer, S., Lacava, T., Melone, F., Moramarco, T., Wagner, W., Dorigo, W., Matgen, P., Martínez Fernández, J., Llorens, P., Latron, J., Martin, C., Bittelli, M., 2011. Soil moisture estimation through ASCAT and AMSR-e sensors: an inter-comparison and validation study across Europe. *Remote Sens. Environ.* 116, 3390–3408.
- Bureau of Meteorology, 2016. Mangalore Airport monthly rainfall.
- Bureau of Meteorology, 2016a. Yanco Agricultural Institute monthly lowest temperature and monthly highest temperature.
- Bureau of Meteorology, 2016b. Peak Hill Post Office monthly lowest temperature and monthly highest temperature.
- Bureau of Meteorology, 2016c. Walkamin Research Station monthly lowest temperature and monthly highest temperature.
- Bureau of Meteorology, 2016d. Charters Towers Airport monthly lowest temperature and monthly highest temperature.
- Bureau of Meteorology, 2012. Climate classification maps: Köppen major classes.
- Choudhury, B.J., Blanchard, B.J., 1983. Simulating soil water recession coefficients for agricultural watersheds. *Am. Wat. Resour.* 19 (2), 241–247.
- Cleverly, J., 2011. Alice Springs Mulga Ozflux Site Ozflux: Australian and New Zealand flux research and monitoring network.
- Crow, W.T., Bindlish, R., Jackson, T.J., 2005. The added value of spaceborne passive microwave soil moisture retrievals for forecasting rainfall-runoff partitioning. *Geophys. Res. Lett.* 32, L18401.
- CSIRO, 2015. Australian cosmic-ray neutron soil moisture monitoring network. accessed 17/03/2015.
- De Jeu, R.A.M., Wagner, W., Holmes, T.R.H., Dolman, A.J., Van de Giesen, N.C., Friesen, J., 2008. Global soil moisture patterns observed by space borne microwave radiometers and scatterometers. *Surv. Geophys.* 29, 399–420.
- Desilets, D., Zreda, M., Ferre, T.P.A., 2010. Nature's neutron probe: land surface hydrology at an elusive scale with cosmic rays. *Water Resour. Res.* 46. <http://dx.doi.org/10.1029/2009wr008726>.
- Dharssi, I., Bovis, K.J., Macpherson, B., Jones, C.P., 2011. Operational assimilation of ASCAT surface soil wetness at the Met office. *Hydrol. Earth Syst. Sci.* 15, 2729–2746.
- Dorigo, W.A., Gruber, A., De Jeu, R.A.M., Wagner, W., Stacke, T., Loew, A., Albergel, C., Brocca, L., Chung, D., Parinussa, R.M., Kidd, R., 2015. Evaluation of the ESA CCI soil moisture product using ground-based observations. *Remote Sens. Environ.* 162, 380–395.
- Draper, C.S., Walker, J.P., Steinle, P.J., De Jeu, R.A.M., Holmes, T.R.H., 2009. An evaluation of AMSR-e derived soil moisture over Australia. *Remote Sens. Environ.* 113, 703–710.
- Draper, C.S., 2011. Near-surface Soil Moisture Assimilation in NWP. University of Melbourne Australia. Doctor of Philosophy Thesis
- Escorihuela, M.J., Chanzy, A., Wigneron, J.P., Kerr, Y.H., 2010. Effective soil moisture sampling depth of L-band radiometry: a case study. *Remote Sens. Environ.* 114, 995–1001.
- Finkele, K., Mills, G.A., Beard, G., Jones, D.A., 2006. National daily gridded soil moisture deficit and drought factors for use in prediction of forest fire danger index in Australia. *BMRC Research Report* no. 119.
- Franz, T.E., Zreda, M., Ferre, T.P.A., Rosolem, R., Zweck, C., Stillman, S., Zeng, X., Shuttleworth, W.J., 2012. Measurement depth of the cosmic ray soil moisture probe affected by hydrogen from various sources. *Water Resour. Res.* 48, W08515.
- Frost, A.J., Ramchurn, A., Hafeez, M., Zhao, F., Haverd, V., Beringer, J., Briggs, P., 2015. Evaluation of AWRA-I: the Australian water resource assessment model. 21st International Congress on Modelling and Simulation 29 November to 4 December 2015
- Haverd, V., Raupach, M.R., Briggs, P.R., Canadell, J.G., Isaac, P., Pickett-Heaps, C., Roxburgh, S.H., Van Gorsel, E., Viscarra Rossel, R.A., Wang, Z., 2013. Multiple observation types reduce uncertainty in Australia's terrestrial carbon and water cycles. *Biogeosciences* 10, 2011–2040.
- Haverd, V., Cuntz, M., 2010. Soil-litter-iso: a one-dimensional model for coupled transport of heat, water and stable isotopes in soil with a litter layer and root extraction. *J. Hyd.* 388, 438–455.
- Hawdon, A., McJannet, D., Wallace, J., 2014. Calibration and correction procedures for cosmic-ray neutron soil moisture probes located across Australia. *Water Resour. Res.* 50, 5029–5043.
- Imaoka, K., Kachi, M., Fujii, H., Murakami, H., Hori, M., Ono, A., Igarashi, T., Nakagawa, K., Oki, T., Honda, Y., Shimoda, H., 2010. Global Change Observation Mission (GCOM) for monitoring carbon, water cycles and climate change. *Proc. IEEE* 98 (5), 717–734.
- Jackson, T.J., Bindlish, R., Cosh, M.H., Zhao, T., Starks, P.J., Bosch, D.D., Seyfried, M., Moran, M.S., Goodrich, D.C., Kerr, Y.H., Leroux, D., 2012. Validation of soil moisture and ocean salinity (SMOS) soil moisture over watershed networks in the U.S. *IEEE Trans. Geos. Rem. Sens.* 50 (5), 1530–1543.
- Jackson, T.J., Cosh, M.H., Bindlish, R., Starks, P.J., Bosch, D.D., Seyfried, M., Goodrich, D.C., Moran, M.S., Du, J., 2010. Validation of advanced microwave scanning radiometer soil moisture products. *IEEE Trans. Geos. Rem. Sens.* 48 (12), 4256–4272.
- Jones, D.A., Wang, W., Fawcett, R., 2009. High quality spatial climate data sets for Australia. *Aust. Meteor., Ocean., J.* 58, 233–248.
- Keetch, J.J., Byram, G.M., 1968. A drought index for forest fire control. Research Paper SE-38 U.S.D.A Department of Agriculture Forest Service.
- Kerr, Y.H., Waldteufel, P., Richaume, P., Wigneron, J.P., Ferrazzoli, P., Mahmoodi, A., Al Bitar, A., Cabot, F., Gruhier, C., Enache Juglea, S., Leroux, D., Mialon, A., Delwart, S., 2012. The SMOS soil moisture retrieval algorithm. *IEEE Trans. Geos. Rem. Sens.* 50 (5), 1384–1403.
- Kerr, Y.H., Wigneron, J.P., Boutin, J., Escorihuela, M.J., Font, J., Reul, N., Gruhier, C., Enache Juglea, S., Drinkwater, M.R., Hahne, A., Martiñ-Neira, M., Mecklenburg, S., 2010. The SMOS mission: new tool for monitoring key elements of the global water cycle. *Proc. IEEE* 98 (5), 666–687.
- Kim, S., Liu, Y.Y., Johnson, F.M., Parinussa, R.M., Sharma, A., 2015. A global comparison of alternate AMSR2 soil moisture products: why do they differ? *Remote Sens. Environ.* 161, 43–62.
- Kohler, M.A., Linsley, R.K., 1951. Predicting the Runoff From Storm Rainfall. U.S. Weather Bureau, Washington D.C.
- Kumar, V., Dharssi, I., Bally, J., Steinle, P., McJannet, D., Walker, J., 2016. Verification of soil moisture from multiple models over Australia for fire danger rating application. *Water Resour. Res.* (in press).
- Lei, F., Crow, W.T., Shen, H., Parinussa, R.M., Holmes, T.R., 2015. The impact of local acquisition time on the accuracy of microwave surface soil moisture retrievals over the contiguous United States. *Remote Sens.* 7, 13448–13465.
- Liu, Y., Van Dijk, A.I.J.M., De Jeu, R.A.M., Holmes, T., 2009. An analysis of spatiotemporal variations of soil and vegetation moisture from a 29-year satellite-derived data set over mainland Australia. *Water Resour. Res.* 45, W07405.
- Liu, Y., De Jeu, R.A.M., Van Dijk, A.I.J.M., Owe, M., 2007. TRMM-TMI satellite observed soil moisture and vegetation density (1998–2005) show strong connection with El Niño in eastern Australia. *Geophys. Res. Lett.* 34, L15401. <http://dx.doi.org/10.1029/2007GL030311>.
- Loew, A., 2014. Terrestrial satellite records for climate studies: how long is long enough? A test case for the Sahel. *Theor. Appl. Climatol.* 115, 427–440.
- Maeda, T., Taniguchi, Y., 2013. Descriptions of GCOM-W1 AMSR2 Level 1R and Level 2 Algorithms. Japan Aerospace Exploration Agency Earth Observation Research Centre.
- Meesters, G.C., De Jeu, R.A.M., Owe, M., 2005. Analytical derivation of the vegetation optical depth from the microwave polarisation difference index. *IEEE Geos. Rem. Sens. Lett.* 2 (2), 121–123.
- Merlin, O., Walker, J.P., Panciera, R., Young, R., Kalma, J., Kim, E., 2007. Soil moisture measurement in heterogeneous terrain. In: Oxley, L., Kulasiri, D. (Eds.), MOD-SIM 2007 International Congress on Modelling and Simulation, Modelling and Simulation Society of Australia and New Zealand. pp. 2604–2610.
- Mladenova, I., Lakshmi, V., Jackson, T.J., Walker, J.P., Merlin, O., De Jeu, R.A.M., 2011. Validation of AMSR-e soil moisture using l-band airborne radiometer data from National Airborne Field Experiment 2006. *Remote Sens. Environ.* 115, 2096–2103.
- Mount, A.B., 1972. The derivation and testing of a soil dryness index using runoff data. *Tasmanian Forestry Commission Bulletin* No. , pp. 4.
- Naeimi, V., Scipal, K., Bartalis, S.H., Wagner, W., 2009. An improved soil moisture retrieval algorithm for ERS and METOP scatterometer observations. *47 (7)*, 1999–2013.
- Northcote, K.H., Beckmann, G.G., Bettenay, E., Churchward, H.M., Van Dijk, D.C., Dimmock, G.M., Hubble, G.D., Isbell, R.F., McArthur, W.M., Murtha, G.G., Nicolls, K.D., Paton, T.R., Thompson, C.H., Webb, A.A., Wright, M.J., 1960. Atlas of Australian Soils, Sheets 1 to 10 With Explanatory Data. CSIRO Australia and Melbourne University Press, Melbourne.
- Northcote, K.H., Hubble, G.D., Isbell, R.F., Thompson, C.H., Bettenay, E., 1975. A Description of Australian Soils. CSIRO Australia.
- Owe, M., De Jeu, R., Holmes, T., 2008. Multisensor historical climatology of satellite-derived global land surface moisture. *J. Geophys. Res.* 113, F01002.
- Owe, M., De Jeu, R.A.M., Walker, J., 2001. A methodology for surface soil moisture and vegetation optical depth retrieval using the microwave polarization difference index. *IEEE Trans. Geos. Rem. Sens.* 39 (8), 1643–1654.

- Panciera, R., Walker, J.P., Jackson, T.J., Gray, D.A., Tanase, M.A., Ryu, D., Monerris, A., Yardley, H., Rudiger, C., Wu, X., Gao, Y., Hacker, J.M., 2014. The Soil Moisture Active Passive Experiments (SMAPEX): toward soil moisture retrieval from the SMAP mission. *IEEE Trans. Geos. Rem. Sens.* 52, 490–507.
- Parinussa, R.M., Holmes, T.R.H., Wanders, N., Dorigo, W., De Jeu, R.A.M., 2015. A preliminary study toward consistent soil moisture from AMSR2. *J. Hydrometeor.* 16, 932–947.
- Pozzi, W., Sheffield, J., Stefanski, R., Cripe, D., Pulwarty, R., Vogt, J.V., Heim, R.R., Jr., Brewer, M.J., Svoboda, M., Westerhoff, R., Van Dijk, A.I.J.M., Lloyd-Hughes, B., Pappenberger, F., Werner, M., Dutra, E., Wetterhall, F., Wagner, W., Schubert, S., Mo, K., Nicholson, M., Bettio, L., Nunez, L., Van Beek, R., Bierkens, M., Goncalves de Goncalves, L.G., Zell de Mattos, J.G., Lawford, R., 2013. Toward global drought early warning capability: expanding international cooperation for the development of a framework for monitoring and forecasting. *Am. Meteorol. Soc.* 94 (6), 776–785.
- Raupach, M.R., Briggs, P.R., Haverd, V., King, E.A., Paget, M., Trudinger, C.M., 2009. Australian Water Availability Project (AWAP): CSIRO Marine and Atmospheric Research Component: final report for phase 3. CAWCR Technical Report No. 013.
- Reichle, R.H., Koster, R.D., Dong, J., Berg, A.A., 2004. Global soil moisture from satellite observations, land surface models, and ground data: implications for data assimilation. *J. Hydrometeorol.* 5, 430–442.
- Renzullo, L., Van Dijk, A.I.J.M., Perraud, J.M., Collins, D., Henderson, B., Jin, H., Smith, A.B., McJannet, D.L., 2014. Continental satellite soil moisture data assimilation improves root-zone moisture analysis for water resources assessment. *J. Hydrol.* 519, 2747–2762.
- Rodell, M., Houser, P.R., Jambor, U., Gottschalk, J., Mitchell, K., Meng, C.J., Arsenault, K., Cosgrove, B., Radakovich, J., Bosilovich, M., Entin, J.K., Walker, J.P., Lohmann, D., Toll, D., 2004. The global land data assimilation system. *Bull. Am. Meteorol. Soc.* 85, 381–394.
- Schmugge, T.J., 1983. Remote sensing of soil moisture: recent advances. *IEEE Trans. Geosci. Rem. Sens.* GE-21 (3), 336–344.
- Schroder, I., 2014. Arcturus Emerald Ozflux Tower Site Ozflux: Australian and New Zealand flux research and monitoring Hdl: 102.100.100/14249.
- Seneviratne, S.I., Corti, T., Davin, E.L., Hirschi, M., Jaeger, E.B., Lehner, I., Orlowsky, B., Teuling, A.J., 2010. Investigating soil moisture-climate interactions in a changing climate: a review. *Earth Sci. Reviews* 99, 125–161.
- Smith, A.B., Walker, J.P., Western, A.W., Young, R.L., Ellett, K.M., Pipunic, R.C., Grayson, R.B., Siriwidena, L., Chiew, F.H.S., Richter, H., 2012. The Murrumbidgee soil moisture monitoring network data set. *Water Resour. Res.* 48, W07701.
- Stenson, M.P., Fitch, P., Vleeshouwer, J., Frost, A.J., Bai, Q., Lerat, J., Leighton, B., Knapp, S., Warren, G., Van Dijk, A.I.J.M., Bacon, D., Pena Arancibia, J.L., Manser, P., Shoesmith, J., 2011. Operationalising the Australian Water Resources Assessment system. . Water Information Research and Development Alliance Science Symposium Proceedings
- Su, C.H., Ryu, D., Young, R.L., Western, A.W., Wagner, W., 2013. Inter-comparison of microwave satellite soil moisture retrievals over the Murrumbidgee basin southeast Australia. *Remote Sens. Environ.* 134, 1–11.
- Taylor, C.M., De Jeu, R.A.M., Guichard, F., Harries, P.P., Dorigo, W.A., 2012. Afternoon rain more likely over drier soils. *Nature* 489, 423–426.
- Van der Schalie, R., Kerr, Y.H., Wigneron, J.P., Rodríguez-Fernández, N.J., Al-Yaari, A., De Jeu, R.A.M., 2016. Global SMOS soil moisture retrievals from the land parameter retrieval model. *Int. J. Appl. Earth Obs. Geoinf.* 45, 125–134. Part B.
- Van der Schalie, R., Parinussa, R.M., Renzullo, L., Van Dijk, A.I.J.M., Su, C.H., De Jeu, R.A.M., 2015. SMOS soil moisture retrievals using the land parameter retrieval model: evaluation over the Murrumbidgee Catchment, southeast Australia. *Remote Sens. Environ.* 163, 70–79.
- Van Dijk, A.I.J., Yebra, M., Cary, G., 2015. A Model-data Fusion Framework for Estimating Fuel Properties, Vegetation Growth Carbon Storage and the Water Balance at Hillslope Scale: Feasibility Study in Namadgi National Park ACT. Bushfire and Natural Hazards CRC, Australia.
- Van Dijk, A.I.J.M., Beck, H.E., Crosbie, R.S., De Jeu, R.A.M., Liu, Y.Y., Podger, G.M., Timbal, B., Viney, N.R., 2013. The Millennium Drought in southeast Australia (2001–2009): natural and human causes and implications for water resources, ecosystems, economy and society. *Water Resour. Res.* 49, 1040–1057.
- Vaze, J., Viney, N., Stenson, M., Renzullo, L., Van Dijk, A., Dutta, D., Crosbie, R., Lerat, J., Penton, D., Vleeshouwer, J., Peeters, L., Teng, J., Kim, S., Hughes, J., Dawes, W., Zhang, Y., Leighton, B., Perraud, J.M., Joehnk, K., Yang, A., Wang, B., Frost, A., Elmahdi, A., Smith, A., Daamen, C., 2013. The Australian Water Resources Assessment Modelling System (AWRA). 20th International Congress on Modelling and Simulation, Adelaide, Australia 1–6 December 2013. pp. 3015–3021.
- Verhoest, N.E.C., Lievens, H., Wagner, W., Alvarez-Mozos, J., Moran, M.S., Mattia, F., 2008. On the soil roughness parameterization problem in soil moisture retrieval of bare surfaces from synthetic aperture radar. *Sensors* 8, 4213–4248.
- Viney, N., Vaze, J., Crosbie, R., Wang, B., Dawes, W., Frost, A., 2015. AWRA-L V5.0: Technical Description of Model Algorithms and Inputs. CSIRO, Australia.
- Viney, N.R., Vaze, J., Vleeshouwer, J., Yang, A., Van Dijk, A., Frost, A., 2014. The AWRA modelling system. *Hydrol. Water Resour. Symp.* 1018–1025.
- Vinnikov, K.Y., Robock, A., Qiu, S., Entin, J.K., 1999. Optimal design of surface networks for observation of soil moisture. *J. Geophys. Res.* 104 (D16), 19743–19749.
- Vreugdenhil, M., Dorigo, W.A., Wagner, W., De Jeu, R.A.M., Hahn, S., Van Marle, M.J.E., 2016. Analyzing the vegetation parameterization in the TU-wien ASCAT soil moisture retrieval. *IEEE Trans. Geosci. Rem. Sens.* 54 (6), 3513–3531.
- Wagner, W., Hahn, S., Kidd, R., Melzer, T., Bartalis, Z., Hasenauer, S., Figa-Salda na, J., de Rosnay, P., Jann, A., Schneider, S., Komma, J., Kubu, G., Brugger, K., Aubrecht, C., Züger, J., Gangkofner, U., Kienberger, S., Brocca, L., Wang, Y., Blöschl, G., Eitzinger, J., Steinnocher, K., Zeil, P., Rubel, F., 2013. The ASCAT soil moisture product: a review of its specifications, validation results and emerging applications. *meteo z.* 22 (1), 5–33.
- Wagner, W., Lemoine, G., Rott, H., 1999. A method for estimating soil moisture from ERS scatterometer and soil data. *Remote Sens. Environ.* 70, 191–207.
- Wagner, W., Lemoine, G., Borgeaud, M., Rott, H., 1999a. A study of vegetation cover effects on ERS scatterometer data. *IEEE Trans. Geosci. Rem. Sens.* 37 (2), 938–948.
- Wanders, N., Karssenber, D., de Roo, A., de Jong, S.M., Bierkens, M.F.P., 2014. The suitability of remotely sensed soil moisture for improving operational flood forecasting. *Hydrol. Earth Syst. Sci.* 18, 2343–2357.
- Wang, Y.P., Houlton, B.Z., Field, C.B., 2007. A model of biogeochemical cycles of carbon, nitrogen, and phosphorus including symbiotic nitrogen fixation and phosphatase production. *Global Biogeochem. Cycles* 21, <http://dx.doi.org/10.1029/2006GB002797>.
- Wang, J.R., Schmugge, T.J., 1980. An empirical model for the complex dielectric permittivity of soil as a function of water content. *IEEE Trans. Geosci. Rem. Sens.* 18, 288–295.
- Wigneron, J.P., Kerr, Y., Waldteufel, P., Saleh, K., Escorihuela, M.J., Richaume, P., Ferrazzoli, P., de Rosnay, P., Gurney, R., Calvet, J.C., Grant, J.P., Guglielmetti, M., Hornbuckle, B., Mätzler, C., Pellarin, T., Schwank, M., 2007. L-band microwave emission of the biosphere (I-MEB) model: description and calibration against experimental data sets over crop fields. *Rem. Sens. Environ.* 107, 639–655.
- Yee, M., Walker, J.P., Dumedah, G., Monerris, A., Rudiger, C., 2013. Towards land surface model validation from using satellite retrieved soil moisture. 20th International Conference on Modelling and Simulation, Adelaide, Australia.
- Zreda, M., Desilets, D., Ferré, T.P.A., Scott, R.L., 2008. Measuring soil moisture content non-invasively at intermediate spatial scale using cosmic-ray neutrons. *Geophys. Res. Lett.* 35, L21402.